Review article

Recent advances in carbon monoxide-releasing nanomaterials☆

Xiaomei Ning [a,c], Xinyuan Zhu [a], Youfu Wang [a,*], Jinghui Yang [b,**]

[a] School of Chemistry and Chemical Engineering, Shanghai Jiao Tong University, Shanghai, 200240, China
[b] Department of Organ Transplantation, Shanghai Changzheng Hospital, Naval Medical University, Shanghai, 200003, China
[c] School of Resources, Environment and Materials, Guangxi University, Nanning, 530004, China

A B S T R A C T

As an endogenous signaling molecule, carbon monoxide (CO) has emerged as an increasingly promising option regarding as gas therapy due to its positive pharmacological effects in various diseases. Owing to the gaseous nature and potential toxicity, it is particularly important to modulate the CO release dosages and targeted locations to elucidate the biological mechanisms of CO and facilitate its clinical applications. Based on these, diverse CO-releasing molecules (CORMs) have been developed for controlled release of CO in biological systems. However, practical applications of these CORMs are limited by several disadvantages including low stability, poor solubility, weak releasing controllability, random diffusion, and potential toxicity. In light of rapid developments and diverse advantages of nanomedicine, abundant nanomaterials releasing CO in controlled ways have been developed for therapeutic purposes across various diseases. Due to their nanoscale sizes, diversified compositions and modified surfaces, vast CO-releasing nanomaterials (CORNMs) have been constructed and exhibited controlled CO release in specific locations under various stimuli with better pharmacokinetics and pharmacodynamics. In this review, we present the recent progress in CORNMs according to their compositions. Following a concise introduction to CO therapy, CORMs and CORNMs, the representative research progress of CORNMs constructed from organic nanostructures, hybrid nanomaterials, inorganic nanomaterials, and nanocomposites is elaborated. The basic properties of these CORNMs, such as active components, CO releasing mechanisms, detection methods, and therapeutic applications, are discussed in detail and listed in a table. Finally, we explore and discuss the prospects and challenges associated with utilizing nanomaterials for biological CO release.

1. Introduction

Gas transmitters, including carbon monoxide (CO), nitric oxide (NO), hydrogen sulfide (H₂S), and oxygen (O₂), play crucial roles in cellular signal transduction [1–3]. They all perform a variety of physiological functions, including regulating blood vessel tone, modulating cell proliferation, mitigating inflammation, and exerting varied effects against pathophysiological processes [4–6]. Thus, gas therapies using these gases as drugs have received increasing attention, especially for various neural diseases [7–9]. As one of the endogenous gas transmitters, CO with a stable structure mainly binds to hemoglobin to regulate cellular functions, such as redox regulation, gene modulation, and enzyme reactions [10–12]. CO exerts its biological effects primarily through several signaling pathways, including regulation of mammalian transcription factor NPAS2 to inhibit heme synthesis and maintain heme homeostasis; activation of P38 mitogen-activated protein kinase for cytoprotection, anti-inflammatory, anti-apoptotic, and anti-proliferative effects; modulation of c-Jun N-terminal kinase (JNK) signaling pathway to suppress pro-inflammatory mediators production; generation of

intracellular second messenger molecule cGMP by binding to guanylate cyclase's active site in physiological processes such as vasodilation and neuronal signal transduction; direct interaction with calcium-dependent potassium channels for inducing vasodilation and regulating vasoconstriction [13]. CO in high concentrations displaces the oxygen in hemoglobin and form carboxyhemoglobin (COHb) to hinder the delivery of oxygen throughout the body, leading to decreased tissue oxygen pressure and organ hypoxia [14–16]. The elevated concentration of COHb in the tissue can lead to symptoms such as dyspnea, coma, syncope, and potentially fatal outcomes [17–19]. In accordance with the model, there exists a correlation between serum COHb levels and the severity of CO poisoning, thereby indicating the severity of associated symptoms. The ratio of serum COHb levels to total hemoglobin is employed for diagnosing the extent of CO poisoning. However, CO at appropriate concentrations provides significant therapeutic effects encompassing antifibrotic, antioxidant, antiapoptotic, antiproliferative, antithrombotic, anti-inflammatory and vasodilatory effects [20–25]. Currently, CO therapy has emerged as a rising gas therapy for diverse diseases. To realize the potential of CO as a therapeutic agent, it is

crucial to develop strategies for targeted delivery of CO to diseased tissues while minimizing the formation of elevated and toxic levels of COHb in the bloodstream.

Due to the gaseous nature and potential toxicity of CO, modulating the dosage of released CO at specific locations is particularly important to elucidate the biological mechanisms of CO and facilitate its clinical applications [26–29]. Therefore, various CO-releasing molecules (CORMs), including metal carbonyl complexes and organic compounds that can release CO in biological systems under some stimuli (light, pH, temperature, etc.), have been developed [30–33]. Metal carbonyl complexes are based on the flexible coordination of CO with metal ions, such as $Fe(CO)_5$, $Mn_2(CO)_{10}$ (CORM-1), $[Ru(CO)_3Cl_2]_2$ (CORM-2), tricarbonyl chloride (glycine) ruthenium (II) (CORM-3), ALF492, CORM-401 which have undergone continuous iterative development to enhance water solubility, stability, responsiveness, and biocompatibility [34]. However, concerns regarding the inevitable toxicity of metal residues persist. Organic CORMs have also garnered attention due to their low toxicity and extensive functionalization options. Examples include CORM-A1, methylene chloride (MC), BW-CO-201~205. It is worth noting that there are fewer types of organic CO donor skeletons available as well as a limited number of responsive release systems. Thus, several limitations hinder the clinical applications of these CORMs, including: (1) low solubility and stability, (2) potential toxicity from the residual metal fragments, (3) inadequate targeted enrichment due to random diffusion, and (4) unpredictable dosage caused by uncontrolled release [11,31,32].

Leveraging the rapid advancements and diverse benefits of nanomedicine, which integrates nanotechnology with biomedicine, controlled-release nanomaterials have been developed for various therapeutic applications to address the limitations associated with CORMs. CO-releasing nanomaterials (CORNMs) possess several advantages, including: (1) their nanoscale dimensions enable high loading capacity, escape from biological barriers, and passive targeted enrichment [35–38], (2) their diverse compositions promote stability, responsiveness, biocompatibility, and degradability [39–41], and (3) their modified surfaces facilitate dispersibility, targetability and multifunctionality (combined therapy and theranostics) [41–43]. Additionally, the cytotoxicity can be reduced by removing any remaining metal residues or fragments together with the CORNMs following CO release [44]. Due to their large drug loading capacity, excellent biocompatibility, enhanced biological enrichment, lengthy release half-life, and high safety, CORNMs have garnered much interest and have undergone rapid development [45–47].

In this review, the applications of various CORNMs in controlling CO release are described in detail based on the latest advances in this field. We provide an overview of CORNMs, which fall within several categories, including organic nanostructures (assembled molecular CORMs, polymeric CORMs, peptides and proteins), hybrid nanomaterials (mainly metal organic frameworks, MOFs), inorganic nanomaterials, and nanocomposites. We focus on the preparations and structures of CORNMs, CO release mechanisms, detection techniques, and therapeutic applications (anticancer, antibacterial, cardiovascular, antiinflammation, among others) (Fig. 1). Finally, we conclude by discussing the limitations of the current research and outlining future directions for CORNMs.

2. CORNMs based on organic nanostructures

Organic compounds, encompassing small molecules, polymers, and biomacromolecules, exhibit favorable biocompatibility and exceptional designability for biological applications [48–50]. Leveraging diverse synthetic strategies, facile modification techniques, and supple structures, organic compounds demonstrate versatile assembly behaviors and remarkable loading capacity. Organic compounds with amphipathic
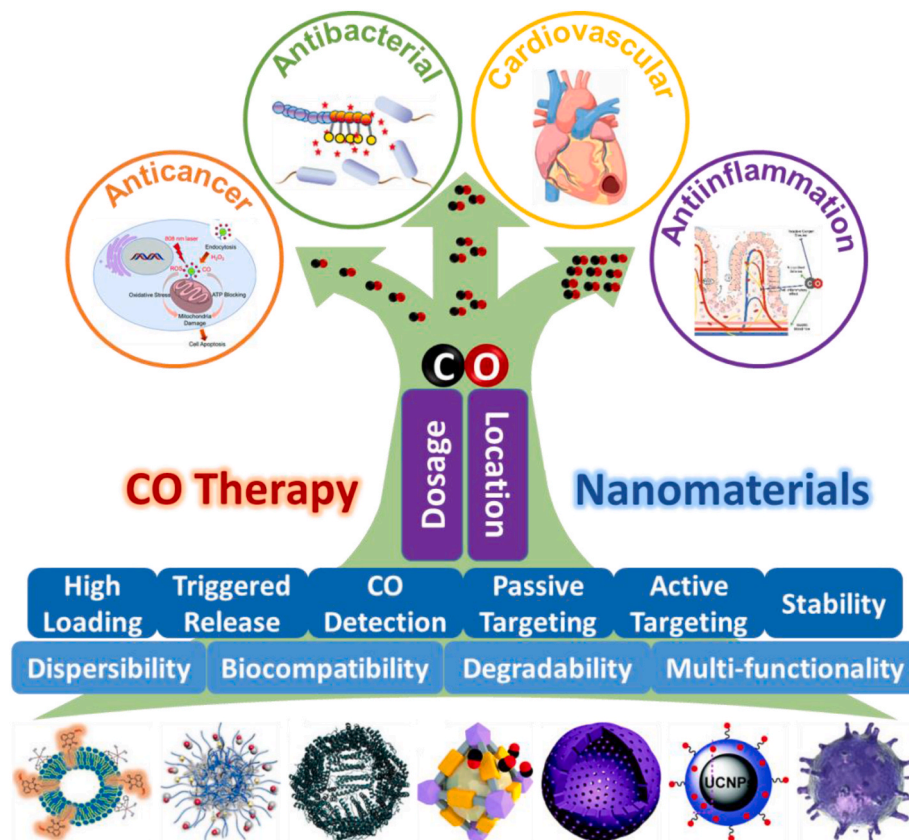

Fig. 1. CO therapy using various nanomaterials with aplenty advantages as CO nanocarriers can control the dosage and location of released CO for varied therapeutic applications.

character can assemble into vesicles and micelles with various nano-structures through intra- and intermolecular interactions. The utilization of organic nanostructures as CO carriers can enhance pharmacokinetics, prolong the half-life of drug release, increase drug loading capacity, and improve solubility, stability and controllability. The combination of CORMs with organic nanostructures exhibits extensive potential for diverse applications. CORMs can be directly encapsulated into organic nanostructures (vesicles, micelles), covalently conjugated with polymers capable of forming nanostructures (nanoparticles, micelles), or bound to peptide or protein nanostructures. The nanoscale organic assemblies also exhibit inadequate structural stability and susceptibility to external factors. Based on the structural characteristics and modes of incorporation of CORMs, it is divided into three categories: 1) CORNMs based on molecular CORMs; 2) CORNMs based on polymeric CORMs; and 3) CORNMs based on peptides and proteins.

2.1. CORNMs based on molecular CORMs

Small molecular CORMs can be directly encapsulated into organic nanostructures, such as vesicles and micelles, through supramolecular interactions. Organic vesicles serve as efficient CO carriers with high loading capacity, good water dispersibility, long CO release half-life, and low biotoxicity. In 2018, D. Amilan Jose et al. developed a nanocarrier that uses vesicles for CO release (Ves-1.Mn) (Fig. 2A) [51]. Since amphiphilic CORMs are easily loaded into lipids, the amphiphilic manganese carbonyl compound, 1.Mn, was assembled with DSPC (phospholipid 1,2-distearoyl-sn-glycero-3-phosphocholine), and then CO-releasing vesicles were obtained through a one-pot method. This CO-releasing vesicle exhibits a sustained release of CO over a 50-min period, with a half-life of 26.5 min, when exposed to light irradiation at 365 nm [52]. The MTT cytotoxicity assay demonstrated excellent biocompatibility of this vesicle both prior to and following CO release. Recently, D. Amilan Jose et al. have made further advancements in the development of a light-activated nanoscale vesicle capable of simultaneous CO release and sensing. (Fig. 2B) [53]. By introducing a sensing probe, N-hexadecyl-3-nitronaphthalimide (NP), and the aforementioned CORM, 1.Mn into the vesicle from DPPC (1,2-dipalmitoyl-sn-glycero-3-phosphocholine), the CO sensing and release system Ves-NP-CO was obtained. The average diameter of Ves-NP-CO is approximately 125 nm, and it can generate CO upon light exposure. The mechanism of the sensing probe relies on the electron-withdrawing properties of the nitro group that induce weak fluorescence. Upon interaction with CO, the 3-nitro group within NP undergoes reduction to an amino group, leading to enhanced fluorescence emission at a peak wavelength of 520 nm. Consequently, Ves-NP-CO enables simultaneous CO release and monitoring.

In 2020, Yingfeng Tu, Yangyan Li and Yao Sun et al. developed a smart CO nanosensor with high selectivity, accuracy and recyclability (Fig. 2C) [54]. They introduced a 4-nitronaphthalimide derivative into a nanochannel with a large opening of 480 nm and a small opening of approximately 18 nm to obtain the CO nanosensor with reversibility and stability. The nitro group within the CO nanosensor can undergo reversible reduction or oxidation by introducing CO from CORM-3 and H_2O_2, leading to reversible changes in fluorescence and surface charge. By manipulating the levels of CO and H_2O_2, the sensor exhibits modulations in ion gating, ion current rectification, and fluorescence signals. This versatile system not only enables precise detection of CO but also demonstrates excellent security features and reversibility, thus holding great promise for future applications and research endeavors.

To explore a new release strategy, Yi Liao and others have also developed a CO-releasing micelle consisting of a pluronic F127 shell, FDA approved polymer, and a core of CORM-2 for CO delivery (Fig. 2D) [55]. The presence of cysteine induces the release of CO from micelles, and this release is further enhanced by ultrasound stimulation. Ultrasound exposure causes the rupture of micelles, thereby exposing enclosed CORM-2 and facilitating its effective interaction with cysteine. The rate of CO release from ultrasound-treated micelles is three times higher compared to untreated micelles. Utilizing ultrasound-mediated delivery of CORM-2-loaded micelles demonstrates a significant reduction in prostate cancer cell proliferation. The incorporation of pluronic F127 and CORM-2 as active components represents a key advantage of this system, which exhibit great potential for future studies.

By encapsulating $MnBr(CO)_5$ (MnCO) and GdW_{10} nanoparticles (GW) in poly (lactic-*co*-glycolic acid) (PLGA), Zongming Liu et al. created an X-ray-induced CO releasing micelles (GW/MnCO@PLGA) possessing anticancer properties (Fig. 3A) [56]. When the micelle was exposed to X-ray irradiation, the radiosensitizer GW was activated by X-rays, leading to the generation of a potent oxidizing superoxide anion ($O_2^{-\bullet}$). Subsequently, $O_2^{-\bullet}$ competitively displaced the Mn center, causing disruption of the Mn–CO bond and subsequent release of CO. Ultimately, through synergistic action between CO and $O_2^{-\bullet}$, direct DNA damage occurred resulting in growth inhibition of cancer cells. The
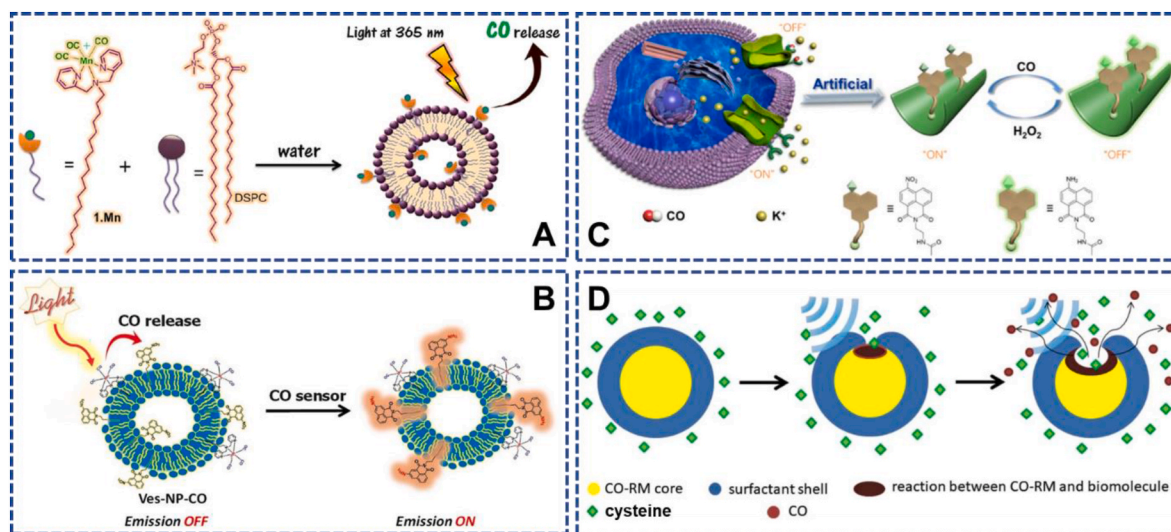

Fig. 2. Organic CORNMs containing molecular CORMs. A) The vesicle containing a light-active CORM for CO delivery [51]. Copyright 2018, ACS. B) The light-active CO vesicle with self-recognition behaviour [53]. Copyright 2023, Elsevier Inc. C) Scheme of a nanochannel-based sensor for CO sensing via a reversible redox reaction strategy [54]. Copyright 2020, ACS. D) A CO-releasing micelle generated CO through the reaction of CORM with regular biomolecules trigged by ultrasound [55]. Copyright 2021, Elsevier B·V.
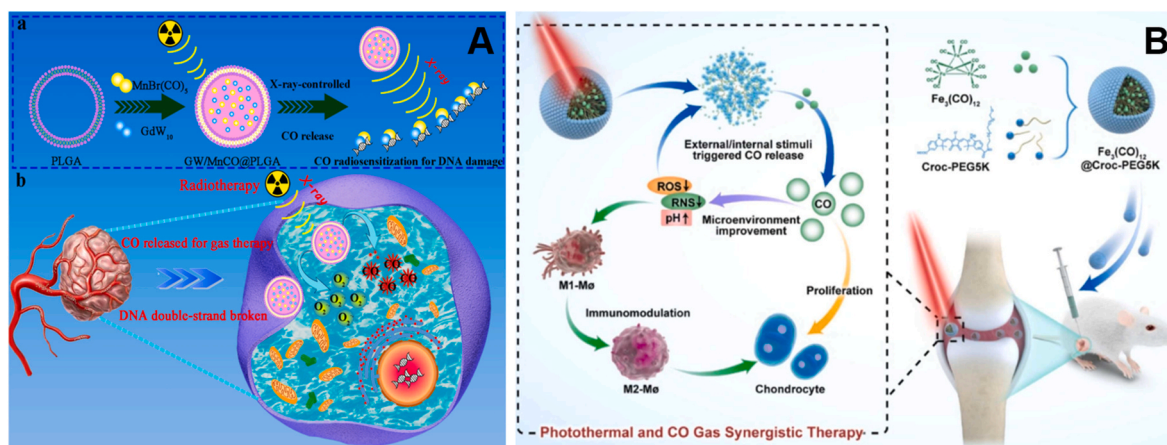
Fig. 3. (A) An X-ray triggered CO-releasing micelles. Schematic illustration of the synthetic strategy and the (a) in vitro and (b) in vivo treatment [56]. Copyright 2022, ACS. (B) Schematic illustration of $Fe_3(CO)_{12}$@Croc-PEG$_{5K}$ for NIR fluorescence imaging-guided photothermal and CO gas synergistic therapy of OA [57]. Copyright 2023, Elsevier.

maximum mortality rate of A549 cells was determined through cell cloning experiments, where a 30-s exposure to X-rays (6 Gy) illuminated the synergistic therapeutic action of CO. Upon reaching a concentration of 100 μg/mL, MnCO exhibited a progressive induction of apoptosis in A549 cells. Furthermore, X-ray-irradiated cells exhibited a higher death rate compared to the non-X-ray group. Based on these results, the combination of radiation therapy (RT) and gas therapy holds promise for cancer treatment.

Huaiyu Wang et al. synthesized a CO delivery system, $Fe_3(CO)_{12}$@Croc-PEG$_{5K}$, by assembling hydrophobic $Fe_3(CO)_{12}$ with an amphiphilic polymer terminated with croconium dye, Croc-PEG$_{5K}$ (Fig. 3B) [57]. Upon NIR laser irradiation (808 nm, 1.0 W/cm^2), the nanomaterial released CO to mitigate the pathological microenvironment of osteoarthritis (OA) through pH regulation in vivo and elimination of free radicals from the OA microenvironment. Simultaneously, the combination of CO gas therapy and pH-dependent NIR fluorescence imaging-guided photothermal therapy (PTT) provided synergistic treatment for OA. Treatment with NIR-irradiated $Fe_3(CO)_{12}$@Croc-PEG$_{5K}$ in LPS-induced RAW264.7 cells resulted in decreased expression of relevant inflammatory factors, indicating effective anti-inflammatory effects. When applied to treat OA in rats, it alleviated the acidic microenvironment and preserved the structural integrity of articular cartilage, demonstrating excellent performance in OA treatment.

2.2. CORNMs based on polymeric CORMs

The construction of polymers with high molecular weights involves the repeated covalent bonding of numerous basic units. [58,59], Polymers, benefiting from diverse synthetic strategies, facile modification and flexible structures, exhibit a wide range of assembled behaviors and possess high loading capacity [60]. The utilization of CORM-conjugated polymers as CO nanocarriers has the potential to enhance pharmacokinetics, prolong release half-life, increase drug loading capacity, and improve dispersibility, stability and controllability, presenting a wide range of promising applications [61].

In 2010, Jeffrey A. Hubbell et al. synthesized amphiphilic polymers to produce CO-releasing micelles with hydrodynamic diameters ranging from 30 to 40 nm [62]. The amphiphilic polymer is a triblock copolymer composed of a poly(ornithine acrylamide) block incorporating Ru$(CO)_3$Cl(ornithine) moieties, a hydrophobic poly(n-butylacrylamide) block, and a hydrophilic poly(ethylene glycol) block. The release of CO from the micelles can be triggered by cysteine or glutathione, with the amount of released CO dependent on the concentration of cysteine/glutathione. Furthermore, it is observed that Ru$(CO)_3$Cl exhibits a

faster release rate compared to that from micelles. These micelles demonstrate enhanced stability in tissues and display targeted therapeutic properties. Additionally, they effectively mitigate NF-κB activation induced by lipopolysaccharide (LPS), along with an enhanced inhibitory effect is observed with increasing concentrations of the micelles, which may be attributed to their ability to reduce inflammation. Moreover, cell viability tests indicate a significant reduction in cytotoxicity associated with the Ru$(CO)_3$Cl(amino acidate) moiety when incorporated into these micelles. This work has showcased the immense potential of polymeric micelles as a safe and effective delivery platform for CO therapy. The use of these micelles not only enhances the therapeutic efficacy of CO therapy but also significantly reduces its potential side effects, making it a promising candidate for various medical applications. As such, further research and development of polymeric micelles as drug delivery systems is warranted, and their potential applications in other therapeutic areas should be explored.

To explore the antimicrobial properties of CO, Cyrille Boyer et al. created a novel water-soluble CO-releasing polymer containing ruthenium carbonyl moieties with resistance to *Pseudomonas aeruginosa* [63]. This polymer can effectively prevent the formation of biofilms, thus, exhibiting greater antibacterial activity and a longer action time than that of CORM-2. In 2020, Yuqin Min and Xinghong Zhang et al. synthesized poly(methyl acrylate) (PMA) centered on diphenyl cyclopropenone (DPCP) [64]. A 365 nm UV light was employed to start the CO release process, and a high-resolution ^{1}H NMR spectrum was used to monitor the photodecarbonization process. They controlled the UV light-triggered CO release process in switching mode and set the timing for UV irradiation to be ON to begin decarbonization and OFF to terminate decarbonization. They also tested the ultrasound-triggered mechanism and showed that the DPCP group at the center of the PMA chain is mechanically stable under ultrasound and that a small amount of water can break the ester bond attached to the DPCP group under ultrasound.

In 2016, U. Hasegawa et al. also developed CO-releasing nanoparticles (CONPs) with anti-inflammatory effects (Fig. 4A) [65]. The polymeric nanoparticles containing phenylboric acid (PBANP) were synthesized by incorporating olefin monomer with phenylboric acid (PBAAM), crosslinker (MBAM), and macromolecular monomer (PEGAM). Subsequently, a ruthenium carbonyl complex with a catechol moiety (CO-DOPA) was conjugated to the PBANP via the high affinity between phenylboric acid and catechol, resulting in the formation of CONPs. The average diameter of the resulting CONPs was 188 nm, and CO-DOPA was loaded onto PBANPs at a molar ratio of 0.7 mol/mol. Notably, the release rate of CO triggered by cysteine from CONPs was slower compared to that from CO-DOPA, with only 40% release
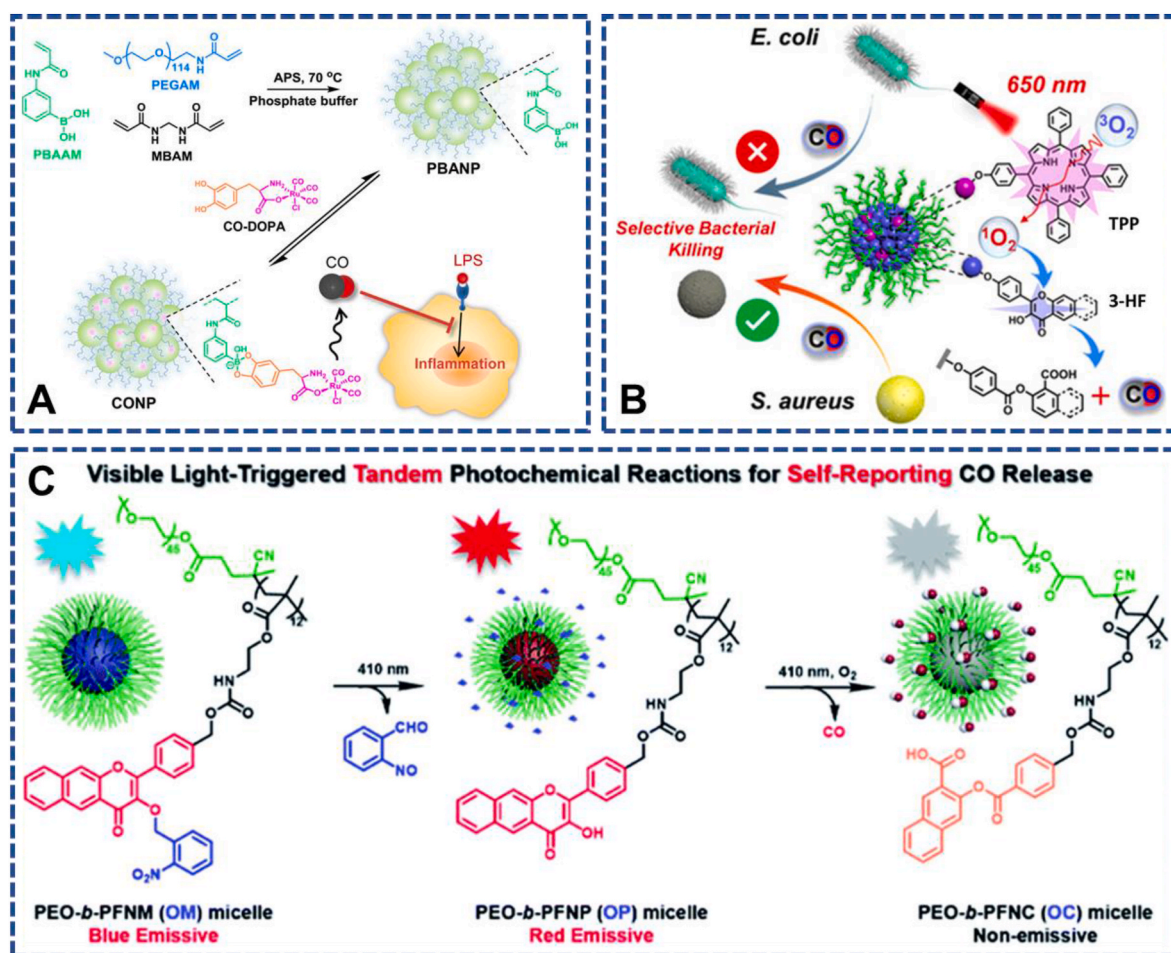
Fig. 4. (A) The synthetic pathway of CONPs and the anti-inflammatory capacity from the sustained release of CO [65]. Copyright 2016, ACS. (B) The micelles containing TPP and 3-HF to trigger CO release under red light and selectively eradicate MRSA infection [66]. Copyright 2021, Wiley-VCH. (C) Self-reporting CO releasing micelles through tandem photochemical processes from blue to red to colorless [67]. Copyright 2020, RSC.

observed after 4 h. The MTT assay conducted on the material using RAW264.7 cells revealed that CO-DOPA exhibited negligible cytotoxicity at concentrations up to 500 μM, whereas cell viability decreased to 70% at concentrations of 1 mM. The anti-inflammatory effect was assessed using RAW264.7 macrophages, and it was observed that CONPs with varying capacities for CO release all demonstrated significant inhibitory effects on LPS-induced inflammation in RAW264.7 macrophages, thereby indicating the potent anti-inflammatory properties of CONPs. The findings of this study hold great promise for the development of novel anti-inflammatory therapeutics based on CONPs. The precise control over CO release and the potent anti-inflammatory effects make CONPs a promising candidate for the treatment of various inflammatory conditions. However, further research is needed to understand the exact mechanism of action and to explore the safety and efficacy of CONPs in vivo.

To extend the wavelength range of light for CO release, Hassan S. Bazzi and Mohammed Al-Hashimi designed a norbornene monomer incorporating a naphthalimide moiety with enhanced long-wavelength absorption and a di-(2-picolyl)amine moiety capable of binding CORMs. Following ring-opening metathesis polymerization (ROMP) of this norbornene monomer, an efficient CO-releasing polymer was obtained [68]. Notably, both the monomer and polymer exhibit exceptional stability in darkness while demonstrating CO release upon exposure to green light. This represents the first reported instance of utilizing green light to trigger CO release in a polymer matrix. By immobilizing the polymer onto PTFE strips, stretchable materials capable of releasing CO can be fabricated.

Furthermore, Jinming Hu et al. successfully incorporated tetraphenylporphyrin (TPP) and 3-hydroxyflavone (3-HF) into the polymeric micelle core with hydrodynamic diameters of approximately 20–60 nm [66]. This micelle can be triggered by red light to release CO. The underlying mechanism involves excitation of TPP photosensitizer under 650 nm light irradiation, leading to conversion of $^3O_2$ to $^1O_2$. Consequently, the oxidization of the encapsulated 3-HF moiety within the micelle core occurs, resulting in efficient CO release (Fig. 4B). Moreover, antibacterial investigations demonstrated that these CO-releasing micelles displayed specific antibacterial effects against *S. aureus* and effectively eradicated methicillin-resistant *S. aureus* (MRSA) bacteria while simultaneously exhibiting hemolytic capabilities that accelerated wound healing in MRSA infections. In an in vitro antibacterial experiment, micelles at a concentration of 0.1 g/L effectively eliminated approximately 97% of MRSA cells within a 30-min duration of light exposure. This study significantly broadens the scope of light-induced CO release by uncovering novel applications and expanding the wavelength range. This breakthrough not only enhances the potential for deep tissue penetration but also paves the way for innovative therapeutic strategies in the field of healthcare. Furthermore, the study delves deep into the intricate mechanisms underlying the antibacterial efficacy, unraveling the crucial role of intracellular CO delivery. This newly discovered role sheds light on the hitherto unknown molecular processes that regulate the antibacterial response, thereby paving the way for the development of novel antibacterial agents. The findings of this study not only expand the existing knowledge base but also hold great potential for the development of innovative therapeutic approaches that can

revolutionize the field of healthcare.

Photodegradable micelles capable of releasing CO under visible light were synthesized by Shenggang Ding, Jinming Hu, and Ruirui Qiao et al. [69]. A prepolymer was obtained through polycondensation of a 3-HF derivative and isophorone diisocyanate (IPDI), followed by capping the ends with hydrophilic poly(ethylene oxide) (PEO). This resulted in the formation of an ABA-type photodegradable triblock copolymer that releases CO. The self-assembly of these triblock copolymers into micellar nanoparticles exhibited a low polydispersity index of 0.189 and an average hydrodynamic radius of 44 nm. These nanomicelles contained *o*-nitrobenzyl ether linkages in their primary chain, which are sensitive to visible light-induced degradation. Upon exposure to continuous light, the *o*-nitrobenzyl ether linkages disintegrate initially, leading to subsequent photooxidation-mediated release of CO from the incorporated 3-HF moiety. The cytotoxicity assessment revealed that micelles at a concentration of 0.2 g/L demonstrated excellent biocompatibility in the absence of light. Remarkably, macrophage-based anti-inflammatory studies demonstrated excellent performance attributed to the light-triggered release of CO from these micelles. This represents the first example of a main-chain degradable micelle system and offers a promising strategy for developing degradable CORNMs.

While post-synthesis modification proves to be an effective technique for constructing CO-releasing polymeric nanomaterials using commercially available polymers, the direct synthesis of CO-releasing polymers offers greater reliability in terms of composition and structure, such as loading or attaching CORMs to the polymer. Guoying Zhang and Jinming Hu et al. developed a CO-releasing micelle from directly polymerized amphiphiles with continuous fluorescence transition (Fig. 4C) [67]. The metal-free CO-releasing amphiphile polymer was prepared through a photoresponsive 3-HF-containing monomer. The micelles formed by the amphiphilic polymer demonstrate excellent aqueous dispersion, exhibiting an average hydrodynamic diameter of approximately 52 nm. The system can initiate a series of photochemical reactions through light irradiation at 410 nm due to the presence of 3-HF derivatives. It can achieve self-reported release of CO through its fluorescence transition from blue to red, ultimately becoming colorless. The cell viability of RAW264.7 cells reached 90% even in the absence of light, at a micelle concentration of 0.2 g/L. In addition to the stable in vitro release of CO measured by MbCO upon illumination, the micelle exhibited fluorescence changes and enabled red fluorescence monitoring for in vivo CO release in mice. Furthermore, they evaluated the anti-inflammatory capacity of these micelles, which demonstrated remarkable performance against LPS-induced TNF-α and nitrite production. These findings emphasize the immense potential of light-triggered CO-releasing micelles as an interesting application for anti-inflammatory purposes and wound healing strategies. The distinctive characteristics of these micelles, including their controlled release of CO gas and targeted delivery, position them as a promising candidate for the development of innovative therapeutics in treating various inflammatory conditions and promoting wound healing.

Alexander Schiller et al. developed a nanoporous nonwoven carrier for CO, where $Mn_2(CO)_{10}$ (CORM-1) is electrospun into the nonwoven fibers without covalent bonding [70]. Upon light-triggered release of CO, the toxic metal residue remains encapsulated within the nonwoven fiber matrix. Cytotoxicity and phototoxicity tests were conducted on 3T3 mouse fibroblasts to evaluate the system's biocompatibility, confirming its low cytotoxicity and strong phototoxicity. By employing a portable CO detector and myoglobin, it was observed that the release rate of CO from nanoporous nonwoven materials exhibited wavelength dependence. The mean CO release from the nanoporous nonwovens was determined to be 3.4 ± 0.3 mol/mg, with four times higher release under 365 nm light compared to 480 nm light. Alexander Schiller et al. conducted further investigations on CO-releasing nanoporous nonwoven materials [71]. They constructed a fiber-based CO release system by embedding manganese tricarbonyl $[(OC)_3Mn(\mu_3\text{-SR})]_4$ (R = nPr) noncovalently into poly(L-Lactide-*co*-D/L-Lactide) and poly(methyl

methacrylate) nonwoven fibers. By leveraging a laser irradiation source, the remote optical triggering at 405 nm wavelength facilitates the precise and controlled release of CO. The amount of released CO is directly proportional to the intensity of the laser beam, ensuring a reliable and consistent delivery. To enhance the precision of this process, the integration of fiber optics with the laser technology is employed. This integration allows for the transmission of CO to the targeted disease site with minimal loss, ensuring that the desired therapeutic concentration is achieved. Moreover, the use of fiber optics provides a safe and efficient means of delivering CO, as it minimizes the risk of accidental exposure and allows for the precise delivery of the gas directly to the site of action. This innovative approach to CO delivery may offer a novel and effective method of treating various diseases.

2.3. CORNMs based on peptides and proteins

Peptides and proteins, as biomacromolecules with exceptional biocompatibility and diverse biological functionalities, have garnered considerable interest as CO nanocarriers. Compared to the direct use of simple CORMs, CORNMs based on peptides and proteins offer enhanced safety, efficiency, and a wider range of features [72–74]. In addition to their low cytotoxicity, biodegradability, and renewability, peptides and proteins can be easily modified while exhibiting remarkable loading capabilities [75–78].

Ulrich Schattschneider et al. successfully conjugated functional Mo $(CO)_4(BPy)$ to a targeting peptide for bioactive transforming growth factor (TGF) using biological orthogonal and catalyst-free oxime connections. The release of CO was detected by myoglobin (MbCO) spectrophotometry [79]. The results demonstrated that the nanocomposite exhibited a slow release of CO when incubated in the dark with a buffer solution. However, under LED irradiation at 468 nm, the rate of CO release significantly increased due to redshifted excitation wavelength compared to the original CORMs, enabling better tissue penetration.

In 2015, Takafumi Ueno et al. successfully developed a series of protein-based CORNMs binding metal carbonyl complexes. The first photoactive protein-based CORNM containing a mutant ferritin (Fr) cage coordinating Mn-carbonyl moieties was developed (Fig. 5A) [80]. The mutant Fr protein cage has an external diameter of 12 nm and is composed of 24 self-assembled polypeptide subunits, in which Fr's Arg52 close to Cys48 was changed to Cys. By attaching the photoactive Mn-carbonyl complex to the protein, Fr-based CORNM containing 48 Mn-carbonyl moieties was obtained. The Mn-carbonyl moieties were stabilized by the formed protein structure. Under 465 nm light, the protein CORNM can slowly release CO and has the effect of activating NF-κB, which is a significant transcriptional control of many genes, such as antiapoptotic genes and proinflammatory genes, and is considered as the therapeutic targets of CO. By altering the duration for which CORNM is exposed to visible light, the amount of releasing CO can be regulated. This discovery marks the very first instance of CORNMs constructed from photoactive proteins. This development signifies a significant leap forward in the field of CORNMs, as it demonstrates the immense potential of protein nanostructures as responsive CORNMs. The versatility of proteins allows for the creation of CORNMs with exquisite temporal and spatial control, opening up a world of possibilities for the precise regulation of CO release.

Takafumi Ueno et al. also developed a protein needle-based CORNM for effective intracellular CO delivery. The protein needle was reconstructed from a cell membrane-puncturing protein 5 of bacteriophage T4 and exhibited excellent permeability and stability. With conjugated CORM-3 $(Ru(CO)_2)$ to the histidine (His) fragment at the protein needle's end (β-PN Ru), a triplet of His-tags containing six histidines is employed at both ends of the protein needle (Fig. 5B) [81]. Compared with that of CORM-3 alone, the release half-life of β-PN Ru was 12 times longer. The helix-shaped center of the protein needle can enhance cell permeability without relying on cell endocytosis. The CORNM demonstrated robust cellular penetration ability and released CO upon reacting
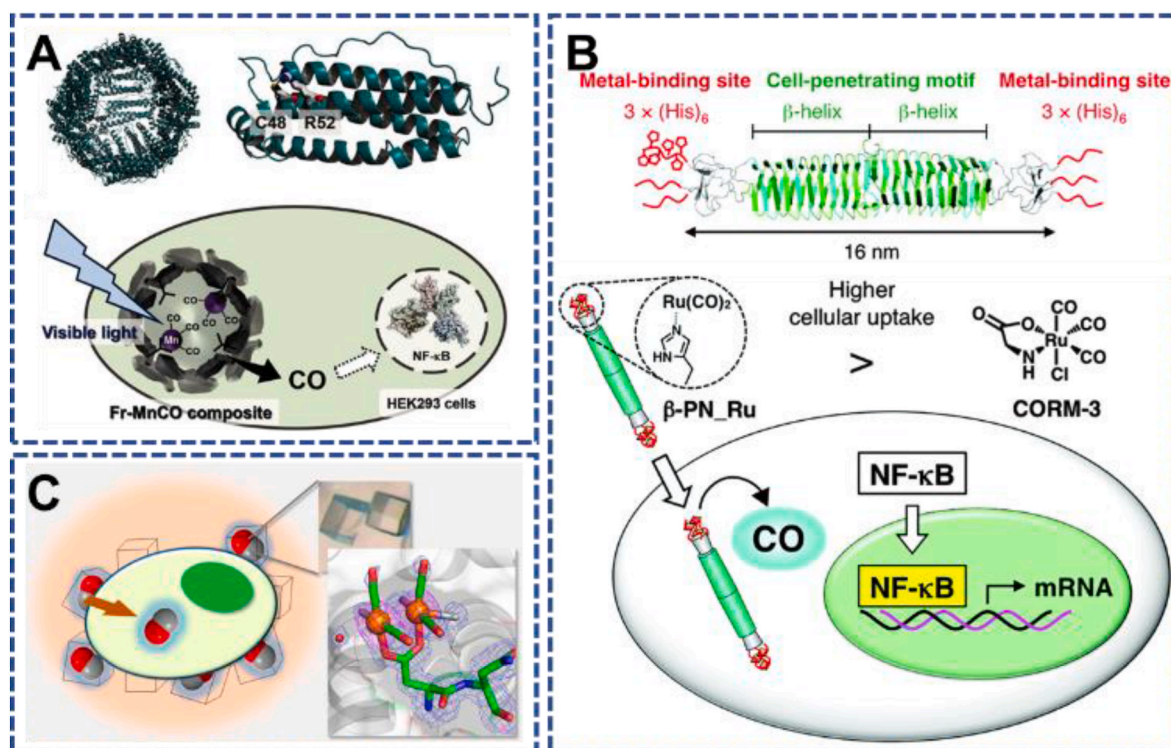
Fig. 5. Protein based CORNMs containing metal carbonyl complexes. A) An intracellular photoactive CORNMs based on mutant ferritin (Fr) cage coordinating Mn-carbonyl moieties for activating NF-κB signaling pathways [80]. Copyright 2016, Wiley-VCH. B) A CORNM based on a Ru carbonyl-protein needle to control NF–B activation [81]. Copyright 2015, RSC. C) A CORNM based on carbonyl ruthenium cross-linked lysozyme crystallization of egg white (Ru·CL-HEWL) [82]. Copyright 2015, ACS.

with endogenous glutathione and cysteine. It exhibited low cytotoxicity and excellent biocompatibility with tissues. Moreover, the protein needle-based CORNM efficiently delivered CO, activating the transcription factor NF-κB and significantly inducing the activity of its target genes HO1, IL-6, and NQO1 through reactive oxygen species (ROS) production. This highlights its remarkable cellular permeability and stability. The emergence of protein-based CORNMs has heralded a significant shift in the field of CORNMs, providing some valuable tools for deciphering complex signaling pathways and propelling innovative medical applications. These novel CORNMs, which integrate the unique properties of proteins with the precision of organometallic synthesis, have the potential to unlock previously unknown insights into CO-related cellular processes and significantly expand our use of CO.

In addition to using protein cages and needles as CORNMs, Takafumi Ueno et al. employed stable cross-linked protein crystals as nanovessels for the containment of metal carbonyl complexes (Fig. 5C) [82]. Crosslinked ruthenium carbonyl hen egg white lysozyme (Ru·CL-HEWL) crystals were synthesized using a ruthenium carbonyl complex as a release agent. STEM-EDX and IR analyses confirmed the even distribution of Ru complexes in Ru·CL-HEWL. X-ray crystallography revealed that each Ru atom was bound to ligand sites (Asp, Lys, His, etc.) with a bond length of 2.2–2.5 Å, consistent with the normal coordination bond length of ruthenium when bonded to amino acids. UV–vis spectrophotometry of MbCO detected consistent CO release from RuCL-HEWL, which significantly improved NF-κB activity. The CO release half-life ($t_{1/2}$) for Ru·CL-HEWL was found to be 19.4 ± 0.8 min compared to approximately ten times longer for CORM-2 under identical circumstances, indicating that Ru·CL-HEWL can serve as an extracellular nanocarrier for efficient CO transport and release in molecular biology studies.

In 2018, Eunji Lee et al. prepared peptide hydrogels (COH) and bioadhesive hydrogel patches (COHP) to release CO (Fig. 6A) [83]. COH is an injectable supramolecular hydrogel with fibrous networks coassembled from CORM-3 connecting a diphenylalanine (FF)-peptide (P2-CORM) and fluorenylmethoxycarbonyl (Fmoc)-FF. COHP patches were produced invoking Fmoc-S, Ca^{2+} and catechol FF with a mussel-inspired COH. Fmoc-S binds Ca^{2+} to COO^- groups, leading to inter-fiber cross-linking and improving the stiffness, rigidity, elasticity and adhesive strength of COHP. Both COH and COHP can be administered intravenously, facilitating precise regulation of the rate of CO release. Additionally, COHP can be delivered via a patch, which exhibits robust mechanical rigidity and excellent adherence properties. Notably, both gels demonstrate efficient CO release for effective suppression of LPS-induced inflammation; furthermore, COH exerts a protective effect on cardiomyocytes. The development of injectable CO-releasing hydrogels represents an innovative approach in the field of regenerative medicine, heralding a novel era of gas transmitters that promise to expand the horizons of biological applications for peptide-based substances. These innovative hydrogels are not just ordinary gel-like materials; they possess a unique biological activity and exhibit supramolecular interactions that significantly enhance their potential uses in various medical settings.

Through the dynamic disulfide bond cross-linking of the biocompatible peptide dendrimer, the formed peptide dendrimer-based nanogel (PDN) has a clear and stable nanostructure and rich expanded voids for effective gust loading. The high reducing condition in disease microenvironment can trigger the cleavage of disulfide bonds and release of guest molecules [86]. Xiaojun Cai et al. developed a CORNM based on PDN integrating the photosensitizer chlorin e6 (Ce6) and H_2O_2-sensitive CORM-401 (Fig. 6B) [84]. Upon NIR light irradiation (665 nm, 25.0 mW cm^{-2}), the photochemical effect mediated by Ce6 not only enhances efficient cellular internalization of the nanogel but also induces rapid intracellular CO release from CORM-401 by depleting H_2O_2 generated during PDT. Importantly, the PDT-driven CO release does not compromise the generation capacity of singlet oxygen ($^1O_2$). Consequently, through concurrent production of substantial quantities of $^1O_2$ and CO
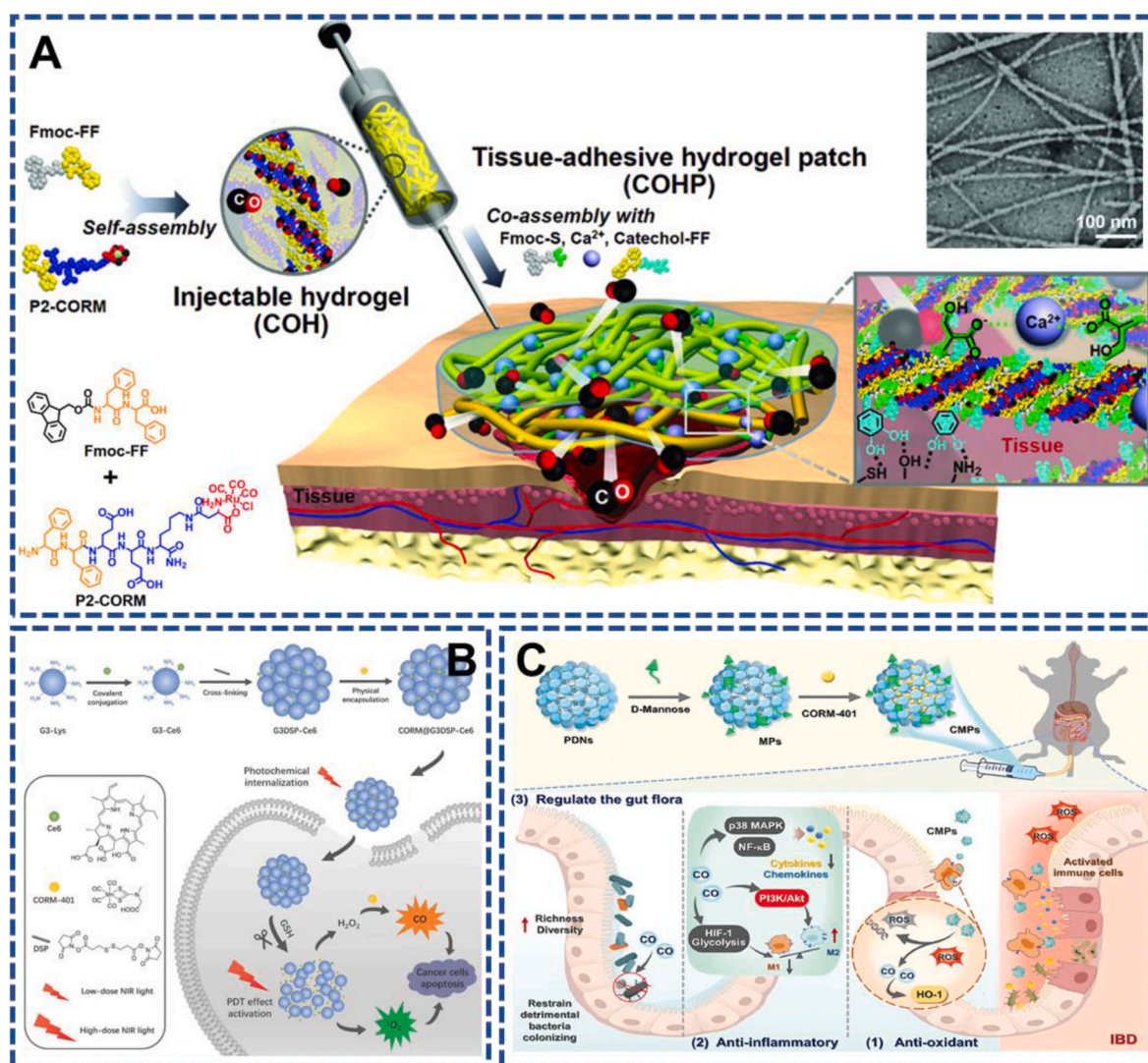
Fig. 6. The diagrammatic representation of the production of injectable supramolecular CO-releasing hydrogel, COH, and the bioadhesive hydrogel patch, COHP [83]. Copyright 2018, Wiley-VCH. (B) PDT-driven highly efficient intracellular delivery and controlled release of CO for synergistic anticancer therapy [84]. Copyright 2018, Wiley-VCH. (C) The preparation and therapeutic mechanism of CMPs to remodel the gut immune-microbiota microenvironment [85]. Copyright 2023, Wiley-VCH.

within cells, the combination therapy of CO and PDT exhibits remarkable synergistic anticancer effects and superior therapeutic safety both in vitro and in vivo. Furthermore, a multi-mode synergistic antibacterial nanoplatform was developed by loading indocyanine green (ICG) and $Mn(CO)_5Br$ onto bipyridine-modified PDN, which can release numerous CO co-driven upon PDT and PTT [87]. The released CO not only facilitates the penetration of ICG into biofilm but also enhances the antibacterial and biofilm eradication effects of PTT and PDT, thereby significantly reducing the inflammatory response induced by bacterial infection, PTT, and PDT. This synergistic antibacterial nanoplatform with excellent biocompatibility demonstrates remarkable efficacy in eliminating urinary tract infections and subcutaneous abscesses.

A multifunctional anti-inflammatory drug named CPHs, PDN encapsulating CORM-401 and wrapping folic acid (FA)-modified hyaluronic acid (HA), was developed for the treatment of osteoarthritis (OA). CPHs effectively target activated macrophages through specific FA and HA-mediated mechanisms, facilitating their entry into these cells. Subsequently, they rapidly release a significant amount of CO by consuming abundant H_2O_2 [88]. In OA joints, CPHs efficiently scavenge ROS levels, thereby effectively inhibiting the degradation of articular cartilage and its extracellular matrix.

A versatile nanomedicine, named CMPs, which are mannose-modified PDN carriers loaded with CORM-401, has been developed for the treatment of inflammatory bowel disease (IBD) (Fig. 6C) [85]. Following rectal administration, CMPs selectively accumulate on the surface of damaged colon mucosa and are subsequently internalized by activated immune cells. By releasing abundant CO induced by high levels of ROS in cells and IBD sites, CORM-401 exhibits diverse therapeutic effects including ROS scavenging, inhibition of inflammation, elimination of pathogens, and relief from colitis. Further research indicates that CMP effectively remodels gut mucosal immune homeostasis and composition of gut flora.

In 2018, albumin based CORNM with high noncovalent affinity with a nonmetallic photoCORM, 3-hydroxybenzo [g]quinolone, was created by Lisa M. Berreau et al. [89] The biocompatibility of the system is enhanced by combining it with serum albumin, enabling targeted administration of CO to cancer cells. Controlled release of CO is triggered by visible light in the nonmetallic CORM-based system. Importantly, no harmful byproducts are generated upon CO release. In vitro cellular studies have demonstrated the effective anticancer and anti-inflammatory performance of this system.

In 2022, Chunmao He and colleagues employed the solid-phase

synthesis strategy to successfully synthesize a series of linear or cyclic peptides featuring azopyridine (azpy) side chains for efficient Mn–CO binding [90]. These Mn–CO-azopyridines encompassed light-responsive peptide motifs capable of CO release upon red light stimulation while preserving the inherent characteristics of the peptides.

3. CORNMs based on hybrid nanomaterials

Hybrid nanomaterials, which combine organic and inorganic components at the atomic or molecular level, fully exploit the advantages of both constituents. Most studies of CORNMs based on hybrid nanomaterials are metal organic frameworks (MOFs), a class of crystalline porous materials formed by coordination between metal nodes and organic linkers [91,92]. Owing to their well-defined structures, MOFs exhibit high sensitivity and excellent drug-carrying capacity [93]. In addition, there are several additional benefits associated with employing MOFs as carriers for CO. Firstly, they offer enhanced CO loading capabilities due to their abundant regular pores and polymetallic sites that provide more binding sites, thereby increasing the amount of loaded CORMs [94–97]. Secondly, MOFs can effectively mitigate metal toxicity by encapsulating and removing residual metals after CO release within their framework structure. Thirdly, the regular pore architecture facilitates rapid and efficient diffusion as well as release of included substances or external media [98–100]. However, MOFs also encounter challenges including inadequate structural stability, potential metal toxicity, and difficulties in surface modification for achieving escape or targeting. Generally speaking, three main strategies are employed for incorporating CORM moieties into MOFs: 1) physical adsorption within nanopores; 2) coordination with metal nodes; and 3) binding with ligands through coordinate or covalent bonds [101–103].

Due to the exceptional performance of MOF systems, they have become extensively investigated materials. Keli Zhong et al. devised a nanodrug delivery system (DDS) (Fig. 7A) for tumor chemotherapy and CO gas therapy [104]. They encapsulated a manganese carbonyl complex (MnCO) and the anticancer drug camptothecin (CPT) within a zeolite-type MOF (ZIF-8), resulting in the formation of a stable DDS named ZCM. ZC and ZM were also prepared by encapsulating CPT or MnCO within ZIF-8, respectively. The size of ZCM particles was approximately 100 nm (Fig. 7A–a), with CPT and MnCO loadings at 14.6% and 17.8%, respectively. Under acidic conditions specific to tumor microenvironments, ZCM decomposed and released CPT along with MnCO as therapeutic agents (Fig. 7A–c). CPT acts as a chemotherapeutic agent that generates substantial amounts of H_2O_2 to eradicate tumors, while MnCO reacts with H_2O_2 to generate CO which exerts detrimental effects on tumors reflecting in their higher ROS content (Fig. 7A–b) compared with ZC and ZM. The FL-Co-1+$PdCl_2$ fluorescent probe was employed for detecting CO levels within the tumor tissue samples obtained from mice models bearing CT26 tumors during antitumor tests mediated by ZCM administration. The synergistic combination of CPT and MnCO within ZCM effectively facilitated CO production in situ within the tumor site itself. Encouragingly, experimental results from CT26 tumor-bearing mouse models demonstrated that the utilization of ZCM exhibited remarkable antitumor efficacy alongside minimal toxicity (Fig. 7A–d).

In 2017, Barea and C. R. Maldonado et al. developed a CO release system for Zn-based MOFs [108]. By incorporating Mo(CNCMe$_2$CO$_2$H)$_3$(CO)$_3$ (ALF794) into the structural pore of [Zn$_2$(dhtp)] (dhtp = 2,5-dihydroxyp-phthalate), h-ZnCPO, a novel one-pot synthesis approach was employed to obtain a CO release system. This system retains the photoactivity of ALF794 and releases CO upon photoactivation.
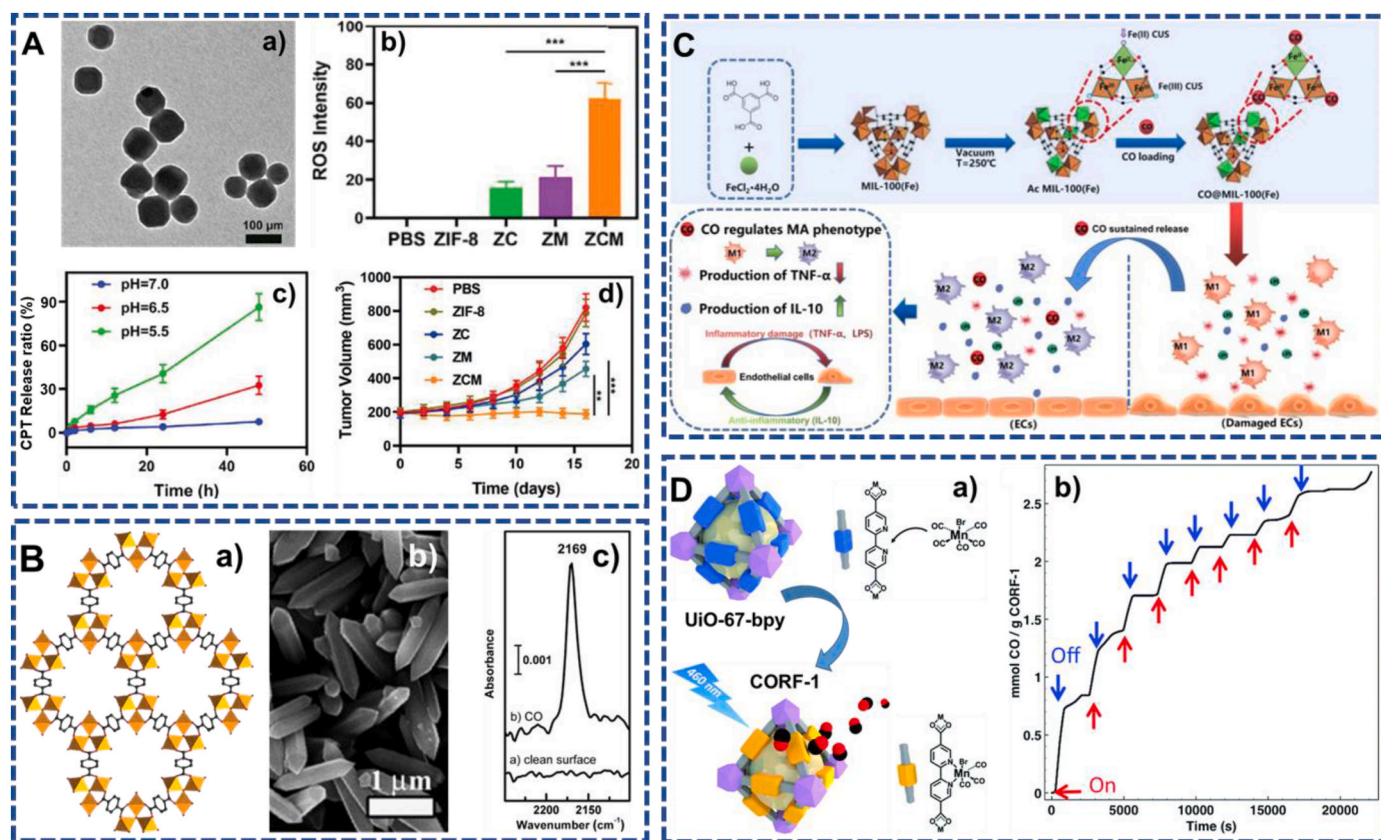

Fig. 7. (A) A novel H_2O_2-triggered CO release MOF containing CORM and CPT for chemotherapy and gas therapy [104]. Copyright 2021, Frontiers Media S.A. (B) MOF based CORNM through activating the metal notes. a) Structure of MIL-88B, b) SEM micrograph of NH$_2$-MIL-88B, c) UHV-IR spectra of NH$_2$-MIL-88B before and after CO incubation [105], Copyright 2013, Wiley-VCH. (C) Diagrammatic representation of the synthesis of CO@MIL-100(Fe) and the impact of released CO on MA over time [106]. Copyright 2022, ACS. (D) UiO-67-bpy loading MnBr(CO)$_5$ and release CO triggered by light [107]. Copyright 2017, RSC.

The released carbonyl moieties leave residual metal fragments in the MOF, effectively reducing metal toxicity. In 2018, Shuhei Furukawa and Elisa Barea et al. investigated the encapsulation of ALF794 within an aluminium-based MOF, [Al(OH)(SDC)]$_n$, (H$_2$SDC: 4,4′-stilbenedicarboxylic acid), CYCU-3 [109]. By varying reagent concentrations (20, 30, 40, 50, 60 mM), they synthesized CYCU x_y particles with distinct sizes (x: concentrations of reagents; y = modulator/ligand ratio). Among them, CYCU-3 20_0 exhibited instability under loading conditions while CYCU-3 50_5 and CYCU-3 50_50 were selected as representative samples due to their particle size range from small to large. The decomposition temperature increased with particle size. Successful loading of ALF794@CYCU-3 50_50 and ALF794@CYCU-3 50_5 preserved the photoactive characteristics of ALF794 while leaching tests demonstrated that ALF794@CYCU-3 50_50 exhibited superior metal retention ability (75% after 72 h in PBS), showing the potential as a practical CORNM.

The first Zr MOFs were the UiO family, and the first member of the UiO family, UiO-66(Zr), has excellent chemical, thermal, and mechanical stability. Isabel S. Goncalves and Martyn Pillinger et al. developed hafnium-based MOFs (UiO-66(Hf)), taking advantage that Hf is more oxyphilic than Zr and that carbonyl is irreversibly adsorbed in Zr MOFs [110]. By incorporating Mo(CO)$_6$ into UiO-66(Hf), an MOF-based CORNM was prepared with subspherical nanocrystals diameters of 60–100 nm and corresponding Mo loadings of 6.0% and 6.6%. Upon exposure to UV radiation at a wavelength of 365 nm, this composite material released a maximum amount of CO equal to 0.26 mmol/g. The leaching of Mo from this system after light-triggered CO release was quantified using ICP–OES analysis, revealing less than 1% leakage after incubation with HEPES buffer for 6 h. UiO-66(Hf) is a versatile and promising host material for the delivery of therapeutic CO, which has been gaining significant attention in the medical community for its potential applications in various fields. This material is renowned for its ease of synthesis, which makes it a cost-effective option for researchers and clinicians. Additionally, UiO-66(Hf) boasts of porous and stable structures, which are essential properties for any material that aims to be used in medical applications. These structures enable the material to withstand various physiological conditions and maintain its integrity over an extended period.

In 2013, Nils Metzler-Nolte et al. developed CO-releasing iron-based MOFs, MIL-88B and NH$_2$-MIL-88B (Fig. 7B) [105]. MIL-88B and NH$_2$-MIL-88B are constructed using oxygen-centered iron (III) carboxylate trimer building blocks, which are further interconnected via terephthalic acid and 2-aminoterephthalic acid, respectively. In contrast to conventional CO nanocarriers that load CORMs into the skeletons, an activation process was employed in this study to eliminate unbridged ligands from the iron coordination sites, resulting in the formation of coordinatively unsaturated iron sites (CUSs) with high affinity for CO molecules. As a result, activated MIL-88B–Fe and NH$_2$-MIL-88B–Fe exhibit potential as CO carriers, capable of slow release under physiological conditions. Increasing the activation temperature from 450 K to 550 K further eliminated terminal ligands and enhanced the number of CUSs. Notably, NH$_2$-MIL-88B possesses a higher density of binding sites compared to unmodified MIL-88B under identical activation conditions. The release rates of CO from MIL-88B–Fe and NH$_2$-MIL-88B–Fe were measured at 0.36 and 0.69 μmol/mg with half-lives of 38 and 76 min, respectively. This MOF carriers necessitate substantial enhancement and optimization to fully unleash their pharmacological potential for applications in the field of medicine. One of the most effective strategies to enhance their therapeutic utility is to reduce their crystal size to the nanoscale. This can be achieved through advanced synthesis techniques and innovative design approaches.

Yajun Weng and colleagues also successfully synthesized a highly crystalline Fe-based MOF, MIL-100(Fe), in aqueous phase at ambient temperature (Fig. 7C) [106]. Similar to MIL-88B, MIL-100(Fe) produces CUSs under vacuum thermal activation conditions, enabling direct binding of CO molecules. To obtain CO@MIL-100(Fe), the annealed MIL-100(Fe) was loaded with CO. Notably, compared to CO@MIL-100

(Fe) with a release half-life of up to 5 h, MIL-88B demonstrates a shorter half-life for CO release. This discrepancy can be attributed to the reduction of Fe(III) to Fe(II) within the MIL-100(Fe) during annealing process. Furthermore, due to its stronger affinity for coordinating with CO, Fe(II) enhances the loading capacity of CO. The structural integrity of MIL-100(Fe) is more robust and can be preserved in PBS for over a week. However, when compared with MIL-88B–Fe (0.36 μmol/mg) and NH$_2$-MIL-88B–Fe (0.69 μmol/mg), the maximum release amount of CO from CO@MIL-100(Fe) is 14.19 μmol/g. The low amount of CO released may be attributed to the strong coordination affinity between CO and reduced MIL-100(Fe), resulting in some bound CO being unable to dissociate under the current experimental conditions. In vitro biological tests reveal that macrophage (MA)-mediated polarization towards M1 phenotype negatively impacts endothelial cell adhesion and proliferation rates. The continuous release of CO by CO@MIL-100(FE) polarizes MA's M1 phenotype into an anti-inflammatory M2 phenotype while secreting anti-inflammatory substances. This reversal of the inflammatory microenvironment promotes endothelial cell development. Therefore, future investigations should focus on enhancing the biocompatibility of these materials while simultaneously endeavoring to optimize their CO loading capacity and prolonging their release kinetics. By improving their biocompatibility, any potential adverse reactions can be effectively minimized, thus ensuring their safe and effective utilization. Optimizing their CO loading capacity will enable these materials to efficiently deliver the necessary medication or treatment, thereby enhancing the overall therapeutic outcome. Prolonging their release kinetics will allow for a more controlled and sustained release of the medication or treatment, which in turn can help to minimize any potential side effects and ensure that the intended therapeutic effect is achieved. This can be especially beneficial in the case of chronic diseases that require long-term treatment.

The CORM moieties can also be bound to the ligands within MOFs. Susumu Kitagawa and Shuhei Furukawa et al. developed a Zr-based light-responsive CO-releasing MOF, CORF-1 (Fig. 7D) [107]. UiO-67-bpy was prepared using zirconium as the metal node and 2, 2′-bipyridine-4,4′-dicarboxylic acid (BPYDC) as the ligand to obtain ortho-octahedral crystals. The dimensions of UiO-67-bpy can be adjusted within the range of 260 nm to 1 mm utilizing the coordination modulation technique. After coordination with the bipyridine moiety, carbonyl manganese (MnBr(CO)$_5$) was loaded into CORF-1, resulting in the formation of CORF-1 with varying sizes capable of CO release upon 460 nm light stimulation. The average sizes of two UiO-67-bpy systems were investigated, measuring 260 nm and 1200 nm, respectively. The smaller crystals exhibited enhanced loading efficiency of MnBr(CO)$_5$ due to the reduced diffusion path length. Specifically, the first and second loading processes achieved loading efficiencies of 79% and 95%, respectively, for the smaller crystals, while the larger crystals showed a loading efficiency of only 60%. Moreover, the release profiles demonstrated accelerated CO release kinetics and improved photoreleasing efficiency. Smaller-sized CORF-1 exhibited enhanced CO loading efficiency and improved light-triggered release efficiency.

Similarly, through the coordination of MnBr(CO)$_5$ within a titanium- and bpy-based MOF (Ti-MOF), Tianfu Wang, Qianjun He, and their colleagues successfully synthesized the H$_2$O$_2$-driven CORNM, MnCO@Ti-MOF [111]. Ti-MOF was prepared using titanium as the metal node and BPYDC as the ligand to obtain ortho-octahedral crystals. Its structure, similar to that of UiO-67, can significantly improve drug loading due to its large surface area. The Fenton reaction can be initiated by H$_2$O$_2$ to induce the release of CO from manganese carbonyl. Given its abundance in the tumor microenvironment, H$_2$O$_2$ creates endogenous conditions for MnCO-mediated CO liberation. The AGS and HeLa cancer cells were selected for comparative analysis, with the AGS cancer cells exhibiting significantly higher levels of H$_2$O$_2$ compared to the HeLa cells. It was observed that MnCO@Ti-MOF demonstrated enhanced efficacy in killing AGS cancer cells as opposed to HeLa cells. Continuous release of CO from MnCO@Ti-MOF may induce apoptosis in tumor cells,

with the rate of CO release being dependent on the concentration of H_2O_2. Consequently, MnCO@Ti-MOF serves as a material capable of selectively eliminating tumor cells without causing harm to healthy ones.

4. CORNMs based on inorganic nanomaterials

Inorganic nanomaterials encompass a range of substances, including gold nanoparticles, mesoporous silica nanoparticles, carbon nanotubes, and others [112,113]. These materials offer numerous advantages such as low toxicity, facile surface modification and manufacturing processes, high biocompatibility, substantial specific surface area, enhanced permeability, and exceptional drug loading capacity [114]. In the field of therapeutics, inorganic nanoparticles can serve as effective agents either independently or when combined with other therapeutic agents as nanocarriers [115]. The integration of inorganic nanoparticles with CORMs holds promise for the development of potential CORNMs, despite the uncertain safety concerns arising from the prolonged retention of many highly stable inorganic nanomaterials in the body.

Carmen R. Maldonado and Elisa Barea et al. successfully synthesized mesoporous silica-based CORNMs in 2016 [116]. Using a cation exchange strategy, [Mn(tacn)(CO)$_3$]$^+$Br (ALF472), which is photoactive, nontoxic, water-soluble, and air-stable, was encapsulated into three different anionic porous frameworks, two of which were mesoporous silica (SO$_3$H-functionalized MCM-41, SO$_3$H-functionalized SBA-15) and the other one was MOF (NH$_2$(CH$_3$)$_2$)$_2$[Zn$_8$(adeninate)$_4$(BPDC)$_6$]•8DMF•11H$_2$O, (BPDC = 4,4′-biphenyldicarboxylate). By comparison, all of them demonstrate excellent capabilities in releasing CO upon exposure to visible light. The leaching experiment reveals that under

physiological conditions, the leaching rate of ALF472 from the MOF system is remarkably high, indicating its inherent instability. In contrast, the mesoporous silica systems exhibit significantly lower leaching rates of ALF472, suggesting their superior stability and controlled release of CO.

In 2017, Carmen R. Maldonado and Elisa Barea et al. conducted further studies on this mesoporous silica system [117]. By employing a cation exchange technique, they successfully loaded ALF472 into mesoporous silica (Al-MCM-41) nanoparticles, resulting in the production of ALF472@Al-MCM-41 with a hydrodynamic size of 112 ± 23 nm. Additionally, ALF472 and the anticancer drug cisplatin were effectively loaded into Al-MCM-41 using a double encapsulation technique to create ALF472-cisplatin@Al-MCM-41 with a hydrodynamic diameter of 336 ± 50 nm. ALF472-cisplatin@Al-MCM-41 exhibited loadings of 0.45 and 0.12 mmol/g for ALF472 and cisplatin, respectively. Both CORNMs, ALF472@Al-MCM-41 and ALF472-cisplatin@Al-MCM-41, demonstrated light-triggered CO release that was more controllable than CORM alone, with equivalent CO release of 0.25 and 0.11 after 24 h, respectively. The leaching rate of metal fragments from the material remained low even after carbonyl moieties were released; similarly, the leaching rate of cisplatin from ALF472-cisplatin@Al-MCM-41 was also low while exhibiting good synergistic drug loading properties.

A cascaded nanocatalyst (RG-Mn@H) was synthesized by Xiaojun Cai, Yu Chen, and Yuanyi Zheng et al. by loading a H_2O_2-sensitive manganese carbonyl complex (MnCO) and glucose oxidase (GOD) inside biodegradable hollow mesoporous organosilica nanoparticles (HMONs) (Fig. 8A) [118]. By utilizing GOD as a nanopore gate, arginine-glycine-aspartic acid (RGD) was incorporated into the surface engineering of HMONs to selectively target cancer cells exhibiting high
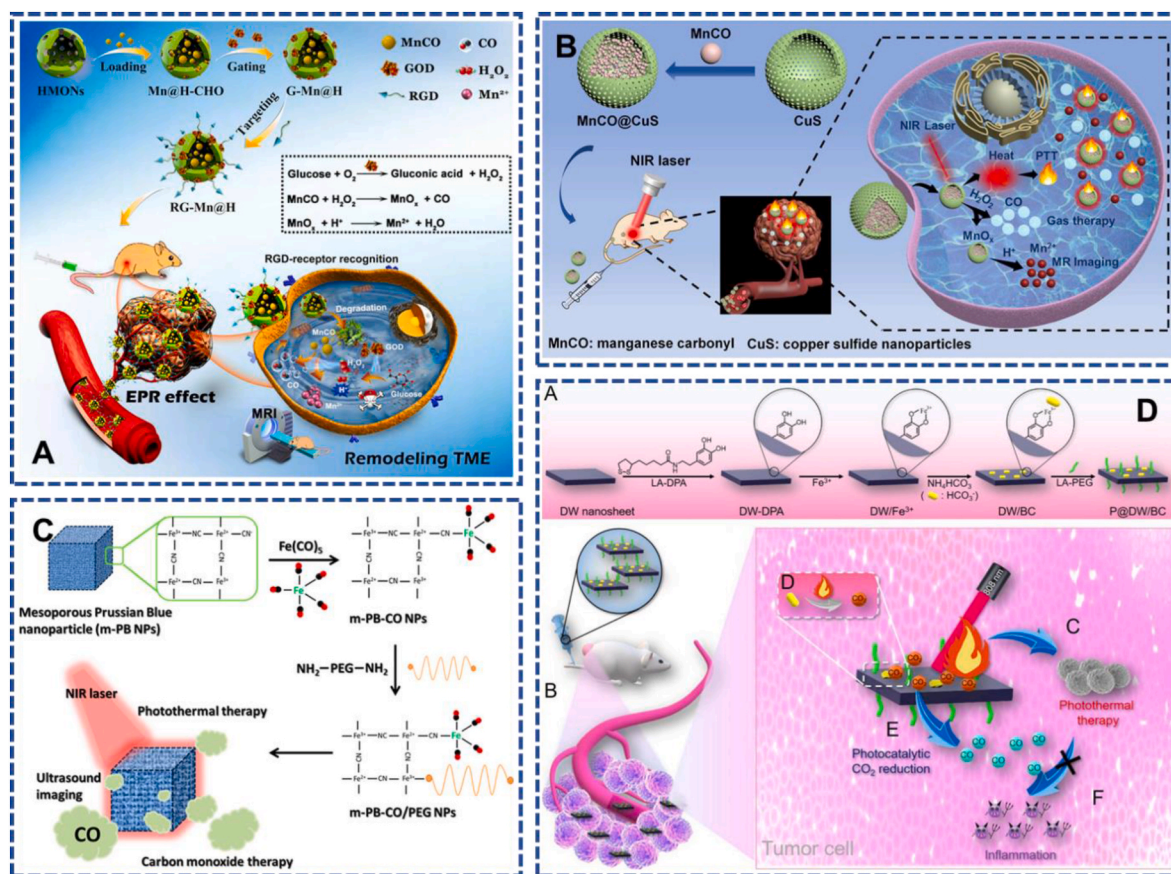

Fig. 8. (A) Diagrammatic representation of the preparation of the cascade nanocatalyst (RG-Mn@H) for remodeling TME [118]. Copyright 2021, Elsevier. (B) Schematic diagram of the preparation of MnCO@CuS NPs with synergistic therapeutic effects of PTT and CO therapy [119]. Copyright 2021, Elsevier. (C) Synthesis of a NIR-responsive m-PB-CO/PEG NPs for PTT, CO release and US imaging [120]. Copyright 2016, ACS. (D) The manufacture of CO-releasing nanosheets P@DW/BC for tumor PTT and anti-inflammation [121]. Copyright 2020, ACS.

αvβ3 expression. The RGD peptide-modified RG-Mn@H demonstrates excellent biocompatibility, intrinsic tumor specificity, and synergistic anticancer effects. The principle underlying the remodeling of the tumor microenvironment (TME) by RG-Mn@H can be summarized as follows: Within the TME, acidic conditions promote GOD dissociation and subsequent release of MnCO. Simultaneously, gluconic acid is generated to impede energy supply and induce cancer cell starvation, thereby facilitating H_2O_2 generation for triggering CO release from MnCO and subsequent TME remodeling. CO can enhance ROS production in cancer cells and induce apoptosis. The anticancer effects of RG-Mn@H on tumor cell apoptosis and its synergistic anticancer effects were validated through both in vitro and in vivo experiments using mouse-derived breast cancer cells.

Other mesoporous inorganic nanomaterials were also prepared as CORNMs. Kai Xu et al. developed MnCO@CuS NPs, a CO delivery nanoplatform, for magnetic resonance imaging (MRI)-guided PTT and CO combined anticancer therapy (Fig. 8B) [119]. They initially synthesized hollow mesoporous CuS nanoparticles (CuS NPs) with uniform sizes, followed by the diffusion of MnCO into the CuS NPs under vacuum conditions to fabricate MnCO@CuS NPs. The photothermal effect induced by NIR laser irradiation at 808 nm from CuS NPs can effectively induce cell apoptosis and photothermal death. MnCO@CuSNPs can increase the temperature to 45 °C at low concentrations (0.1 mg/mL) and low light densities (1.0 W/cm^2) to induce cell apoptosis through PTT. MnCO@CuS NPs, possessing comparable photothermal capabilities to those of CuS NPs, demonstrate positive effects in PTT. Moreover, the combination of H_2O_2 generated within the TME and external laser enables in situ CO release from MnCO@CuS NPs, exhibiting higher efficiency than that achieved solely through NIR or H_2O_2 stimulation. The presence of H_2O_2, photothermal impacts, and acidic environments can also facilitate the degradation of MnOx (MnCO decomposed products), resulting in the generation of free Mn^{2+} for tumor MRI. Through both in vivo and in vitro investigations, it has been demonstrated that the combined application of PTT and CO exhibits synergistic anticancer effects, surpassing those achieved by either PTT or CO treatment alone.

Chen-Sheng Yeh et al. developed a mesoporous nanosystem (m-PB-CO/PEG NP) that exhibits a near-infrared (NIR) light-responsive CO delivery capability (Fig. 8C) [120]. The synthetic process is as follows: (1) synthesis of mesoporous Prussian blue nanoparticles (PB), an FDA-approved remedy for heavy metal poisoning, through a cross-linking process; (2) modification of the PB NPs by coupling Fe(CO)$_5$; and (3) surface chelation with amine-functionalized poly(ethylene glycol) to obtain the m-PB-CO/PEG NPs. UV–vis spectrophotometry was employed to monitor the binding of reduced hemoglobin to CO, enabling tracking of CO release. Precise control over CO release from the nanoparticles was achieved by NIR light treatment, leveraging the gaseous nature of CO for ultrasound imaging (USI). The thermal stability investigation of m-PB-CO/PEG demonstrated CO release at 42 °C, while no release occurred at 37 °C. Irradiation with 808 nm NIR light at intensities of 0.3 W/cm^2 and 0.8 W/cm^2 elevated the solution's temperature to 35 °C and 50 °C respectively. Notably, both CO release and cell ablation were observed at an intensity of 0.8 W/cm^2, whereas only CO release was observed at an intensity of 0.3 W/cm^2. In vitro and in vivo experiments involving m-PB-CO/PEG NPs treated with NIR light at an intensity of 0.8 W/cm^2 revealed enhanced apoptotic and tumor suppressive effects, highlighting their synergistic impact combining PTT and gas therapy for cancer treatment.

Xian-Zheng Zhang et al. synthesized a polyethylene glycol (PEG)-modified bicarbonate (BC)-functionalized defective tungsten oxide (WO$_3$) nanosheet (P@DW/BC) with near-infrared light (NIR) responsiveness. (Fig. 8D) [121]. The synthesis process is as follows: (1) annealing the WO$_3$ atomic layer in a reducing atmosphere to induce oxygen vacancies; (2) sonicating the DW atomic layer in water to convert it into DW nanosheets; (3) modifying the DW nanosheets with lipoic acid-bound dopamine (LA-DPA); (4) utilizing iron ions (Fe^{3+}) as coordinating centers to link DPA and BC; and (5) functionalizing the

nanosheets with PEG to obtain P@DW/BC. Under NIR laser irradiation, P@DW/BC exhibits a remarkable therapeutic effect on tumors. The underlying mechanism of this therapy is as follows: (1) Upon exposure to 808 nm NIR laser, P@DW/BC acts as a proficient photothermal agent and facilitates efficient photothermal conversion for achieving precise PTT. (2) The generated heat from the photothermal conversion effectively disintegrates BC at temperatures exceeding 40 °C, leading to the release of CO$_2$. (3) Subsequently, P@DW/BC serves as an exceptional photocatalyst for converting CO$_2$ into CO, thereby mitigating inflammation induced by PTT. Consequently, through the synergistic effects of PTT and CO generation, tumor growth can be significantly suppressed. This innovative system enables in situ CO generation within tumor tissues, resulting in superior efficacy compared to conventional tumor therapies.

Anke Krueger and Ulrich Schatzschneider et al. developed a CORNM in 2012, utilizing nanodiamond particles as the platform [122]. The modification of nanodiamond involved the adsorption of a manganese carbonyl complex (Mn(CO)$_3$(tpm)$^+$), achieved through a copper-catalyzed click reaction between 1,3-dipole azide and cycloalkyne. The successful determination of myoglobin demonstrated the CO release capability of this system.

In 2020, Isabel S. Goncalves and Martyn Pillinger et al. utilized a one-pot method to introduce ALF795 into zinc, aluminium layered double hydroxide (LDH), resulting in the creation of a light-triggered CO releasing material that retains the photoactive properties of the original CORM while preventing premature dissociation and maintaining potential toxic residual segments within the LDH matrix. After incubation at 37 °C for 5 h and ultraviolet radiation, only 2% of molybdenum was leachable, indicating excellent stability and biocompatibility [123]. This observation highlights the remarkable capability of LDH hosts in effectively preserving both intact CORMs and decarbonylated fragments.

5. CORNMs based on nanocomposites

Despite significant advancements in research on mono-component nanocarrier-based CORNMs, there is an urgent need for the development of CORNMs with multifunctionality and multiple properties, particularly for active targeting, synergistic enhancement, and overcoming physiological barriers. By integrating two or more nanomaterials or nanostructures based on specific requirements, nanocomposites can leverage their respective advantages to achieve diverse functionalities and properties that cater to various application needs. Consequently, nanocomposites with exceptional designability and versatility have gained widespread attention across numerous fields. The preparation processes of nanocomposites are generally complex, leading to increased costs and challenges in achieving structural uniformity, thereby imposing limitations on their further clinical promotion.

In 2013, Peter C. Kunz, Annette M. Schmidt and Christoph Janiak et al. used biocompatible magnetic iron oxide nanoparticles (IONPs) as carriers for CORNMs [124]. The obtained CORNM exhibits the capability of CO release under a magnetic field. In the absence of IONPs, the CO release rate remains unchanged with or without the application of an alternating magnetic field, suggesting that magnetic nanoparticles can potentially serve as local field antennas to induce targeted CO release in tissues.

Furthermore, Matthias U. Kassack and Christoph Janiak et al. developed a CORNM based on maghemite (Fe$_2$O$_3$) IONPs in 2015 (Fig. 9A) [125]. They covalently attached tri(carbonyl)-chloro-phenylalanine-ruthenium (II) complexes onto the surface of IONPs and subsequently coated them with a dextran polymer. To effectively mitigate the interference caused by strongly adsorbed IONP ions on myoglobin, they devised a myoglobin testing method: encapsulating polymer-coated IONPs within hollow calcium alginate spheres and conducting myoglobin tests. By spatially isolating CORM from myoglobin and preventing rapid replacement reactions between
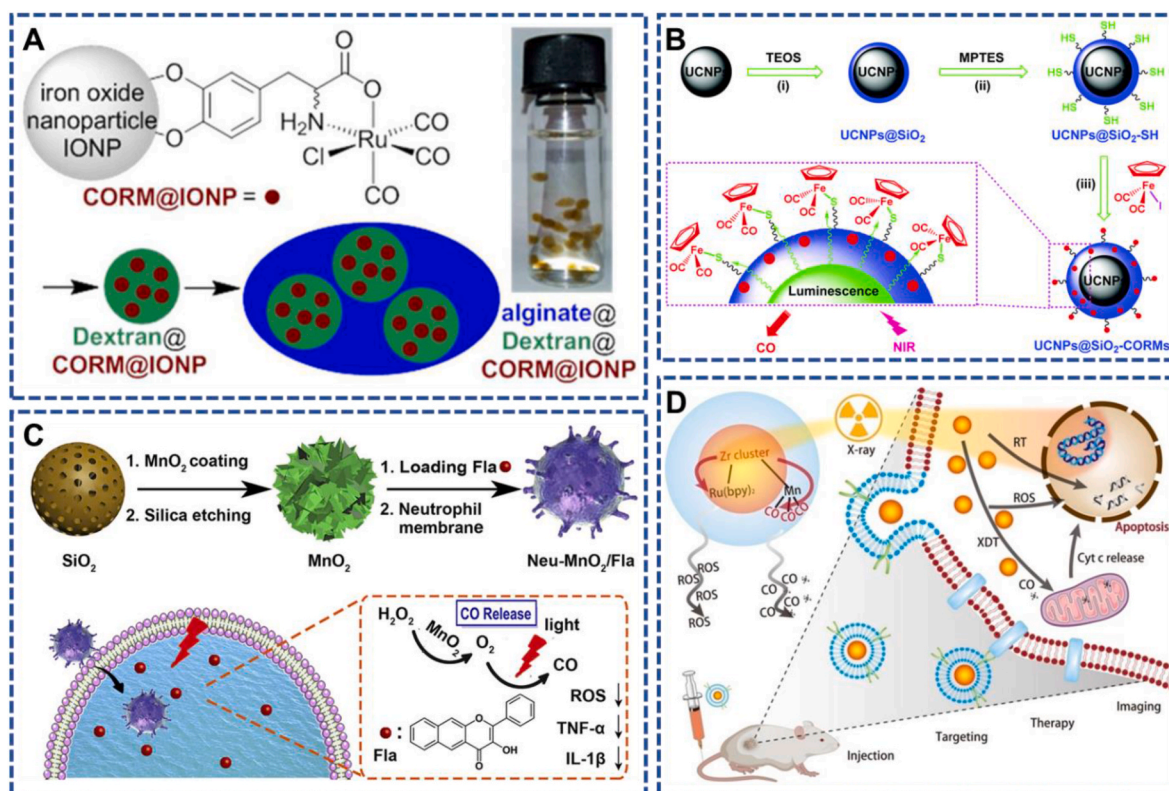
Fig. 9. (A) Preparation of functionalized IONPs and alginate stably spheres for controlled CO release under magnetic field [125]. Copyright 2015, ACS. (B) The preparation of UCNP@SiO₂-CORM, which can release CO triggered by NIR-light [127]. Copyright 2017, RSC. (C) The targeted synergistic anti-inflammation CORNM. up) Synthetic strategy of Neu-MnO₂/Fla; down) Schematic diagram of in-situ targeted synergistic anti-inflammation of CO [128]. Copyright 2020, Elsevier. (D) Schematic illustration of ZrRuMn-MONs@mem for XDT and CO gas therapy [129]. Copyright 2020, Wiley-VCH.

CORM-3 and proteins, the measurement of myoglobin remains unaffected by high absorbance materials such as IONPs. The release of CO is dependent on both time and temperature, with higher temperatures resulting in faster CO release. Furthermore, the release rate of CO can be accelerated by an external alternating magnetic field. Matthias U. Kassack and Christoph Janiak et al. conducted further investigations on this system [126]. CORMs containing oxime groups and a catechol-modified backbone were covalently attached to the surface of maghemite IONPs using a similar experimental approach as described in the previous study. The results demonstrate that the release of CO is also influenced by temperature and the applied magnetic field. Notably, compared to earlier studies, the activation energy at the alginate particle surface decreased from 78 kJ/mol to 62 kJ/mol.

The low toxicity and stability of proteins have garnered increasing attention, yet the rapid drug clearance and nonspecific distribution of most protein-CORM adducts lead to non-sustained drug release. This issue can be addressed by encapsulating CORMs within protective structures. Teresa Santos-Silva and Pedro V. Baptista et al. developed a gold nanoparticle-CORM-3 conjugate [130]. AuNPs@PEG@BSA·Ru(CO)x were synthesized through covalent attachment of ruthenium carbonyl complex (CORM-3) onto bovine serum albumin (BSA), which was conjugated to gold nanoparticles via PEG. The CORNM platform is employed to facilitate nanovectorization, thereby enhancing the efficient cellular uptake of the nanoformulation and subsequently leading to an elevation in intracellular CO levels. Evaluation of the anti-inflammatory properties of this nanoparticle system demonstrated its significant potential for wound healing.

In 2014, Nanfeng Zheng and Peter C. Ford et al. developed a CORNM based on an upconversion nanocomposite [131]. The core of these CORNM nanoparticles consists of ytterbium-doped lanthanide materials as near-infrared absorbers and thulium as visible light emitters, while the nanoparticle surface is coated with an amphiphilic polymer. To

achieve good dispersibility, the manganese carbonyl complex was successfully loaded into the polymer matrix during synthesis. The release of CO by light triggering was facilitated by the nanoparticles. However, due to the opaqueness of human tissue to UV–vis light, achieving effective irradiation of the CORNMs within the tissue is challenging. To overcome this limitation, an upconversion material capable of absorbing multiple long wavelength photons and subsequently emitting a single short wavelength photon was employed. This enables the conversion of near-infrared light into UV–visible light. In 2017, Ran Jiang and Xiaoming Liu et al. also developed an upconverted core-shell structured CORNM for CO release (Fig. 9B) [127]. The homogeneous β-NaYF₄:Yb³⁺/Er³⁺ upconversion nanoparticles were coated with an 8 nm silica shell and subsequently functionalized with 3-mercaptopropyltrimethoxysilane to introduce thiol groups. The UCNP@SiO₂-CORM photo-responsive system was constructed by attaching an iron carbonyl complex (Fe(η₅-Cp)(CO)₂I) onto the surface of CORNM through a ligand exchange reaction with mercaptan groups. The resulting CORNMs exhibited uniform hexagonal morphology with an average diameter of approximately 119 nm. Upon irradiation with 980 nm light, CORNM released CO gas, while maintaining residual iron on its surface due to the strong affinity between thiolates and irons. Human umbilical vein epithelial cells (HUVECs) and mouse fibroblasts (L929) were employed to assess the biocompatibility of UCNPs@SiO₂-CORMs, revealing excellent biocompatibility without any noticeable phototoxicity.

Xiaogang Qu et al. synthesized a CO-releasing nanoplatform, Neu-MnO₂/Fla, with synergistic anti-inflammatory activity (Fig. 9C) [128]. Hollow mesoporous MnO₂ nanoparticles were synthesized by employing MSNs as templates, followed by the mixing of the Mn precursor and MSNs, subsequent heat treatment, and silica etching. To create Neu-MnO₂/Fla, the mesoporous MnO₂ NPs were further functionalized with a coating of neutrophil cell membrane after loading Fla (a small molecule precursor capable of CO release). The coated neutrophil cell

membrane has demonstrated its efficacy and potential as a promising platform for various inflammatory disorders and autoimmune diseases. To achieve in situ light-induced CO release with inflammation-targeted therapeutic capabilities, the proposed mechanism involves the catalytic conversion of H_2O_2 into oxygen by MnO_2-catalyzed catalase in inflamed tissues. Subsequently, under aerobic conditions, Fla exhibits a light-induced response releasing CO. The ability of Neu-MnO_2/Fla to target inflammation was evaluated using PC12 cells. MTT measurements revealed that at experimental doses, Neu-MnO_2/Fla exhibited lower cytotoxicity towards PC12 cells under both nonlight and light conditions. The inflammatory response in PC12 cells was confirmed by assessing the proinflammatory cytokines TNF-α and IL-1β levels. Following LPS treatment, PC12 cells were treated with either Neu-MnO_2 (without Fla) or Neu-MnO_2/Fla with light exposure. Results demonstrated that while Neu-MnO_2 had no significant impact on TNF-α and IL-1β levels, Neu-MnO_2/Fla did exhibit an effect. These findings suggest that compared to Neu-MnO_2 alone, Neu-MnO_2/Fla possesses superior anti-inflammatory performance. Furthermore, when conducting anti-inflammatory tests on mice with inflamed paws, it was observed that under laser irradiation, the ROS levels were lower in the group treated with Neu-MnO_2/Fla compared to the control group without laser irradiation. Based on these results, it can be concluded that at the site of inflammation, Neu-MnO_2/Fla generates sufficiently high concentrations of CO to exert noticeable anti-inflammatory effects due to excess H_2O_2 present in inflamed tissues.

Recently, Chengchao Chu and Gang Liu et al. developed a ruthenium-based metal organic nanostructured (MON) radiosensitizer (ZrRuMnMON@mem) incorporating Zr clusters, Ru(BPy)$_2$, and Mn $(CO)_5$Br to integrate X-ray-induced dynamic therapy (XDT) and CO gas therapy (Fig. 9D) [129]. The combined treatment of XDT and CO gas therapy exhibits synergistic enhancement. Subsequently, the nanoparticles were coated with cell membranes expressing antiglypican 3 (GPC3) antibody (hGC33), enabling active tumor targeting while maintaining biocompatibility. By utilizing Zr as an X-ray absorber in the MON, Ru is stimulated to generate reactive oxygen species (ROS), while MnCO releases CO gas through X-ray energy transfer. The MRI signal of ZrRuMn-MONs is enhanced upon exposure to X-rays, serving as a marker for CO release and allowing real-time in-body monitoring. In vitro evaluation of ZrRuMn-MON@mem and ZrRu-MON@mem was conducted using HepG2 human hepatocellular carcinoma cells and LO2 healthy liver cells. The results demonstrate that membrane-modified MONs by GC33 enhance endocytosis by HepG2 cells, leading to improved targeted therapeutic effects. HepG2 cells internalize more membrane-wrapped MONs compared to LO2 cells. This combined action of CO gas and ROS produces a powerful and efficient cell-killing mechanism, making it a valuable tool in various medical and scientific applications.

6. Summary and outlooks

The primary challenge in utilizing CO as a therapeutic agent lies in the delivery of suitable dosages to targeted locations, necessitating the development of delivery systems with consistent pharmacokinetics that align with the narrow therapeutic window of CO for desired effects [132]. Although various developed CORMs can release CO, they are typically not used alone due to their limited solubility, low stability, potential toxicity, short half-life for CO release [133]. Currently, combining CORMs with different nanocarriers to form CORNMs is a widely employed technique aimed at enhancing solubility/dispersibility, stability, biocompatibility, and release half-life of CORM. Organic nanostructures (such as vesicles, micelles) based on small molecules, polymers, and peptides/proteins, hybrid nanomaterials (primarily MOFs), inorganic nanomaterials, and nanocomposites have been extensively investigated as potential nanocarriers for integrating CORMs [134]. Table 1 provides an overview of the synthesis and fundamental properties of these CORNMs including CO releasing mechanisms and

detection methods. Significant progress has been made in CORNMs research particularly concerning novel release strategies, active/passive targeting techniques, and CO detection methods. Diverse active/passive targeting techniques effectively address the issue of location control for CORNMs; however, dosage control challenges still persist owing to the underlying mechanisms governing CO release along with associated detection methods (Fig. 10) [135,136].
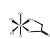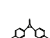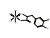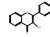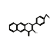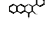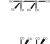
The current CO release strategies mainly involve endogenous factors such as reactive oxygen species (ROS, such as H_2O_2, $^1O_2$, $O_2^{-\bullet}$), microenvironment (cysteine and glutathione) and exogenous factors such as light, ultrasound, magnetic field, X-ray, temperatu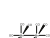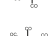re and so on. Light activation is a commonly employed strategy for CO release and has led to numerous significant advancements. However, the inherent phototoxicity and limited light penetration still pose substantial obstacles to its clinical applications. Protein nanocarriers are typically triggered by glutathione and cysteine in vivo, which offers a highly convenient mechanism; however, the control of CO release remains unexplored. Rapid CO release may be imperative for various therapeutic purposes, and ultrasonic or magnetic field activation can expedite this process. Nevertheless, there is currently no research investigating the potential safety risks associated with such rapid CO release. Research on H_2O_2-triggered CO release has gradually garnered attention. The current study on the H_2O_2 triggering mechanism is mostly focused on anticancer due to the high concentration of H_2O_2 in tumor cells [137]; however, the development of additional applications is still needed. Furthermore, alternative mechanisms for CO release exist, including temperature, pH, enzymes, and system-independent CO release, seeing Table 2. However, limited research has been conducted on these aspects. Therefore, there is ample room for further development in exploring other strategies for CO release. Considering the individual variations and diverse stages of disease progression, investigating the precise response to specific microenvironments in different diseases could be a promising avenue of research.

The dosage of CO as a therapeutic agent is the primary determinant affecting its therapeutic efficacy and safety. Therefore, it is crucial to accurately measure the quantity and half-life of CO release. Direct measurement of CO poses challenges due to its gaseous nature. A wide range of techniques, including gas chromatography, chromogenic detection, electrochemical assays, laser sensor-infrared absorption and others, have been devised and developed for the precise detection of CO [138]. However, these methods are currently limited to detecting and imaging physiological concentrations of CO in living cells. The myoglobin method, which detects CO release through absorption spectrum shifts in oxidized myoglobin, is commonly employed for this purpose. The fluorescent probe method holds great promise for in vivo CO detection due to its inherent advantages, including high sensitivity and resolution, real-time observation capability, non-invasive and non-destructive testing.

The mechanism of fluorescent probes for CO sensing is closely related to the coordination of CO with a metal center possessing a labile ligand or available coordination site. Generally, there are two strategies employed for CO sensing using metal complexes: (a) utilizing the metal complex as both a receptor and a signaling unit for CO response; (b) employing the metal complex to catalyze the conversion of weak emissive precursors into strong fluorescent derivatives in the presence of CO. However, it should be noted that one potential drawback associated with fluorescent probes based on metal complexes lies in their potential toxicity [139]. Real-time detection of released CO can be combined with imaging modalities such as ultrasound imaging, photoacoustic imaging, electrochemiluminescence imaging, MRI, etc.

In conclusion, the clinical application of CO-releasing materials will continue to progress steadily. The future research direction for CO-releasing material development remains focused on enhancing safety, precision, manageability, and targeted release of CO.

Table 1
Summary of the properties and applications of CORNMs.

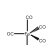|	Nanomaterials	CO donors	CO loading methods	CO release mechanism	Detection method	Dimension	involved cells types	combined or synergistic therapy	animal model	CO donor structure	Targeting	Therapeutic applications	Ref.
vesicle	Ves-1.Mn	Mn(CO)$_5$Br	Chemical modification	365 nm	Myoglobin assay	120–140 nm	C2C12	–	–		–	–	51
vesicle	Ves-NP-CO	Mn(CO)$_5$Br	Physical absorption	365 nm	Probes	125 nm	–	–	–		–	–	53
vesicle	pluronic micelle	CORM-2	Physical absorption	ultrasound	Head space method	109 ± 16 nm	PC-3	–	–		–	Anti-cancer	55
vesicle	GW/MnCO@PLGA	Mn(CO)$_5$Br	Physical absorption	X-Ray (O$_2^{-\bullet}$)	COP-1	155.8 nm	A549	Radiation and CO for tumor	Mouse tumor model		–	RT and CO combined anticancer	56
micelle	CO-releasing micelles	Ru(CO)$_3$Cl	Chemical modification	Cysteine	Myoglobin assay, CO detector	30–40 nm	THP-1 Blue™	–	–		–	Anti-inflammatory	62
polymer	polymer	CORM-2	Chemical modification	Spontaneous	Myoglobin assay	lower than 10 nm	PAO1	–	–		–	antibacterial	63
micelle	DPCP-PMA	diphenyl cyclopropenone	Chemical modification	UV light	PL	–	–	–	–		–	–	64
micelle	CONPs	CORM-3	Chemical modification	Cysteine	Myoglobin assay	188 nm	RAW264.7	–	–		–	Anti-inflammatory	65
polymer	polymer	Mn(CO)$_5$Br	Chemical modification	550 nm	Myoglobin assay	–	HEK	–	–		–	phototherapy bandage	66
micelle	TPP nanomicelles	3-HF	Chemical modification	605 nm (^{1}O$_2$)	portable CO detector	20–60 nm	L929	–	–		Targeted to Staphylococcus aureus	Antibacterial (MRSA)	67
micelle	nanomicelles	3-HF derivatives	Chemical modification	Visible Light	Portable CO detector (DRAGER PAC6500)	44 nm	RAW264.7	–	–		–	Anti-inflammatory	68
micelle	CORPs	3-HF	Chemical modification	visible light	Myoglobin assay	52 nm	RAW264.7	–	murine full-thickness cutaneous wound model		–	Anti-inflammatory	69
micelle	Nanoporous non-wovens	CORM-1	Physical absorption	365–480 nm	Myoglobin assay	fiber about 1 μm	3T3	–	–		–	–	70
micelle	Nanoporous non-wovens	CORM-1	Physical absorption	365 nm and 405 nm	Myoglobin assay	fiber about 1.3–2.1 μm (PLA) and 2.9–5.6 μm (PMMA)	3T3	–	–		–	–	71
Protein	peptide	Mo(CO)$_{4bpy}$	Chemical modification	486 nm	Myoglobin assay	–	–	–	–		–	–	79
Protein	Protein Cage	Mn(CO)$_5$Br	Chemical modification	456 nm	COP-1	12 nm	HEK293	–	–		–	Activation of nuclear factor κB (NF-κB) in cells	80
Protein	β-PN_Ru protein needle	CORM-2	Chemical modification	Glutathione and cysteine	Myoglobin assay	10.7 ± 1.9 nm	HEK293	–	–		–	Activation of nuclear factor κB (NF-κB) in cells	81
Protein	cross-linked hen egg white lysozyme crystals (Ru·CL-HEWL)	CORM-2	Chemical modification	Releases CO under physiological conditions	Myoglobin assay	–	HEK293	–	–		–	Activation of nuclear factor κB (NF-κB) in cells	82
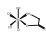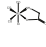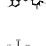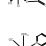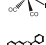
Table 1 (*continued*)

	Nanomaterials	CO donors	CO loading methods	CO release mechanism	Detection method	Dimension	involved cells types	combined or synergistic therapy	animal model	CO donor structure	Targeting	Therapeutic applications	Ref.
Protein	peptide hydrogel	CORM-3	Chemical modification	–	Myoglobin assay	7 nm	H9C2, RAW 264.7	–	–	(structure)	–	Heart protection and anti-inflammatory	83
Protein	peptide nanogel	CORM-401	Physical absorption	H2O2	CO detector (Bosean BH-90A)	180 nm	4T1, L929	PDT & CO for tumor	mice breast tumor	(structure)	–	Anticancer	85
Protein	peptide nanogel	MnBr(CO)$_5$	Chemical modification	PDT, PTT	CO detector	207 nm	HUVECs, L929, RAW264.7	PDT, PTT, CO for biofilm infections	biofilm infection model	(structure)	–	Antibacterial, biofilm	86
Protein	peptide nanogel	CORM-401	Physical absorption	H2O2	CO detector	265 nm	Macrophages	CO for OA	Rat model of OA	(structure)	FA- and HA-mediated targeting	anti-inflammatory	87
Protein	peptide nanogel	CORM-401	Physical absorption	ROS	CO detector	254 ± 11 nm	Macrophages, Caco-2, RAW264.7	CO for inflammatory bowel disease	mouse model of acute colitis	(structure)	–	anti-inflammatory	88
Protein	BSA	quinolone-type photoCORM	Physical absorption	Visible light	Gas chromatography	–	HUVEC, A549, RAW 264.7	–	–	(structure)	–	Anti-cancer and anti-inflammatory	89
Protein	peptide	Mn(CO)$_5$Br	Chemical modification	Red light	Myoglobin assay	–	U87,MCF-7, HeLa,	–	–	(structure)	Targeted CO release	Targeted CO release	90
MOF	ZIF-8	MnCO	Physical absorption	H2O2	FL-Co-1 + PdCl2 fluorescence probe	100 nm	CT26	CT and CO for tumor	Mouse tumor model	–	Passive Targeting	Inhibition of tumors in CT26 mice	104
MOF	ZnCPO	ALF794	Physical absorption	365 nm	Myoglobin assay	–	–	–	–	(structure)	–	Improved residual metal retention	105
MOF	CYCU-3	ALF794	Physical absorption	Visible Light	Myoglobin assay	~100 nm	–	–	–	(structure)	–	Improved residual metal retention	106
MOF	UiO-66(Hf)	Mo(CO)$_6$	Physical absorption	365 nm	Myoglobin assay	60–100 nm	–	–	–	(structure)	–	Improve stability	107
MOF	MIL-88B and NH$_2$-MIL-88B	CO	Chemical absorption	–	Myoglobin assay	MIL-88B: 2.4 μm*1.2 μm NH$_2$-MIL-88B: 1.5 μm*300 nm	–	–	–	–	–	–	108
MOF	MIL-100(Fe)	CO	Chemical absorption	–	fluorescent probe 1-Ac	300~800 nm	endothelial cells (ECs), RAW 264.7	–	–	–	–	Anti-inflammatory	109
MOF	CORF-1	Mn(CO)$_5$Br	coordinate	460 nm	Myoglobin assay	260 nm - 1 μm	HeLa	–	–	(structure)	–	Reduces cytotoxicity	110
MOF	Ti-MOF	Mn(CO)$_5$Br	coordinate	H$_2$O$_2$	Myoglobin assay	–	HeLa, AGS	–	–	(structure)	–	Anti-cancer	111
Inorganic nanomaterials	MCM-41-SO$_3$H and SBA-15-SO$_3$H	[ALF472]$^+$	ion exchange strategy	visible light	Myoglobin assay	–	RAW264.7	–	–	(structure)	–	Improved stability	116
Inorganic nanomaterials	Al-MCM-41	[ALF472]$^+$	ion exchange strategy	visible light	Myoglobin assay	Single envelope: 112 ± 23	–	CO and CT for tumor	–	(structure)	–	Good synergistic drug delivery	117

Table 1 (*continued*)

|	Nanomaterials	CO donors	CO loading methods	CO release mechanism	Detection method	Dimension	involved cells types	combined or synergistic therapy	animal model	CO donor structure	Targeting	Therapeutic applications	Ref.
						nm Double envelope: 336 ± 50 nm							
Inorganic nanomaterials	RG-Mn@H	MnCO	Physical absorption	PH	COP-1 CO fluorescence probe	126.8 nm	L929, MDA-MB-231, 4T1, PC3, HeLa, HCT116	CO and starvation therapy for tumor	MDA-MB-231 breast cancer model	–	Tumor-specific biodegradation	Tumor specificity, synergistic anticancer effects	118
Inorganic nanomaterials	MnCO@CuS NPs	MnCO	Physical absorption	808 nm NIR/H_2O_2	COP-1	124 nm	MV3, HSF	CO and NIR synergize scandium tumors	Mouse tumor model	–	Tumor Specificity	CO and PTT combined anti-cancer	119
Inorganic nanomaterials	m-PB-CO/PEG NPs	$Fe(CO)_5$	Chemical modification	808 nm	Hemoglobin assay	202.5 nm	HeLa	CO & PTT for tumors	Mouse tumor model	[structure]	–	CO and PTT combined anti-cancer	120
Inorganic nanomaterials	P@DW/BC	Bicarbonate	Chemical modification	808 nm	CO Probe	86 nm	CT26	CO & PTT for tumor	Mouse tumor model	–	–	CO and PTT combined anti-cancer and anti-inflammatory	121
Inorganic nanomaterials	Nano-diamond particle	$[Mn(CO)3(tpm)]^+$	Chemical modification	365 nm	Myoglobin assay	10 nm	–	–	–	[structure]	–	–	122
Inorganic nanomaterials	Layered Double Hydroxide	ALF795	Physical absorption	365 nm	Myoglobin assay	100–500 nm	–	–	–	[structure]	–	Improved stability and biocompatibility	119
Nanocomposites	CORM@IONP	CORM-3	Chemical modification	Alternating magnetic field	Myoglobin assay	9 ± 2 nm	–	–	–	[structure]	–	–	124
Nanocomposites	Alginate@Dextran@CORM@IONP	CORM-3	Chemical modification	Magnetic Heating	Myoglobin assay	60–140 nm	A2780, Cal27, HEK293	–	–	[structure]	–	–	125
Nanocomposites	Alginate@Dextran@CORM@IONP	CORM of oxime	Chemical modification	Alternating magnetic field	Myoglobin assay	–	A2780, Cal27, HEK293	–	–	[structure]	–	–	126
Nanocomposites	AuNPs@PEG@BSA·Ru(CO)x	CORM-3	Physical absorption	–	COP-1	73 nm	HCT116,THP-1	–	–	[structure]	–	Anti-inflammatory	127
Nanocomposites	UCNPs	Manganese carbonyl	Chemical modification	365 nm	Myoglobin assay	16–30 nm	–	–	–	[structure]	–	–	128
Nanocomposites	UCNPs@SiO2-CORMs	Fe (Z5-Cp)(CO)2I	Chemical modification	980 nm	IR spectral changes	119 nm	HUVEC, L929	–	–	[structure]	–	Good biocompatibility	129
Nanocomposites	Neu-MnO2/Fla	Fla	Physical absorption	H_2O_2 and light	absorption and emission spectra	244 nm	PC12, Neutrophil	Synergistic anti-inflammatory	Mouse inflammation model	[structure]	Active targeting	Synergistic anti-inflammatory	130
Nanocomposites	ZrRuMnMONs@mem	$Mn(CO)_5Br$	Chemical modification	X-Ray (ROS)	Myoglobin assay	356 nm	LO2, HepG2	XDT and CO for tumor	Mouse HCC tumor model	[structure]	Active targeting	XDT and CO combined anticancer	131
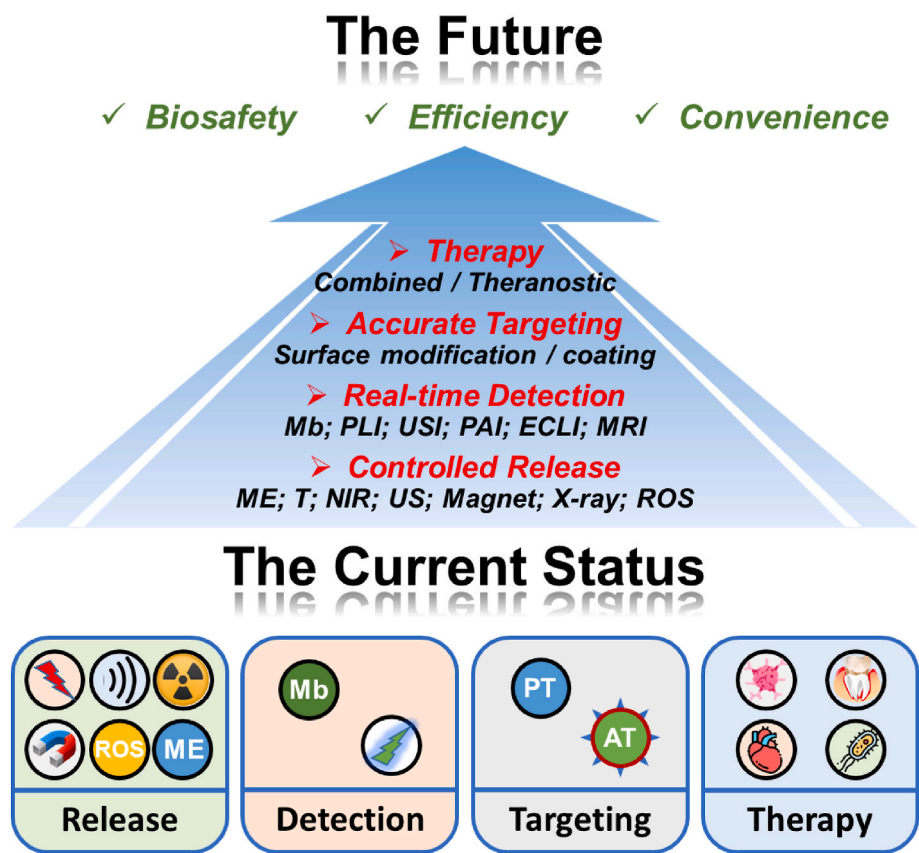
Fig. 10. Current issues involved in CO gas therapy and potential directions for further development.

Table 2
The advantages and disadvantages of various stimulus triggering CO release.

Release Stimulus	Advantages	Disadvantages
Glutathione/ Cysteine	endogeneity	bad site and dose control
ROS	endogeneity, selectivity	bad dose control
pH	endogeneity, selectivity	bad dose control
Light	good site and dose control, collaborating with phototherapy	exogenous, limited penetration depth, phototoxicity
X-ray	good site and dose control, unlimited penetration depth, collaborating with X-ray therapy	exogenous, radiation injury
Magnetic Field	good site control	exogenous, bad dose control

CRediT authorship contribution statement

Xiaomei Ning: Writing – original draft. **Xinyuan Zhu:** Supervision. **Youfu Wang:** Writing – review & editing, Supervision. **Jinghui Yang:** Writing – review & editing.

Declaration of competing interest

The authors declare that they have no known competing financial interests or personal relationships that could have appeared to influence the work reported in this paper.

Acknowledgments

References

[1] Y. Qian, J.B. Matson, Gasotransmitter delivery via self-assembling peptides: treating diseases with natural signaling gases, Adv. Drug Deliv. Rev. 110–111 (2017) 137–156, https://doi.org/10.1016/j.addr.2016.06.017.

[2] W. Gong, C. Xia, Q. He, Therapeutic gas delivery strategies, Nanomed Nanobiotechnol 14 (1) (2022) e1744, https://doi.org/10.1002/wnan.1744.

[3] S.W. Ryter, A.M. Choi, Carbon monoxide: present and future indications for a medical gas, Korean J. Intern. Med. (Engl. Ed.) 28 (2) (2013) 123–140, https://doi.org/10.3904/kjim.2013.28.2.123.

[4] R. Siracusa, V.A. Voltarelli, A.T. Salinaro, S. Modafferi, S. Cuzzocrea, E. J. Calabrese, R. Di Paola, L.E. Otterbein, V. Calabrese, No, co and h(2)s: a trinacrium of bioactive gases in the brain, Biochem. Pharmacol. 202 (2022) 115122, https://doi.org/10.1016/j.bcp.2022.115122.

[5] A. Carne-Sanchez, F.J. Carmona, C. Kim, S. Furukawa, Porous materials as carriers of gasotransmitters towards gas biology and therapeutic applications, Chem. Commun. 56 (68) (2020) 9750–9766, https://doi.org/10.1039/d0cc03740k.

[6] Y. Wang, T. Yang, Q. He, Strategies for engineering advanced nanomedicines for gas therapy of cancer, Natl. Sci. Rev. 7 (9) (2020) 1485–1512, https://doi.org/10.1093/nsr/nwaa034.

[7] A. Ismailova, D. Kuter, D.S. Bohle, I.S. Butler, An overview of the potential therapeutic applications of co-releasing molecules, Bioinorgan. Chem. Appl. 2018 (2018) 8547364, https://doi.org/10.1155/2018/8547364.

[8] C.S. Queiroga, A. Vercelli, H.L. Vieira, Carbon monoxide and the cns: challenges and achievements, Br. J. Pharmacol. 172 (6) (2015) 1533–1545, https://doi.org/10.1111/bph.12729.

[9] Y. Xu, Y. Li, A. Gao, P.K. Chu, H. Wang, Gasotransmitter delivery for bone diseases and regeneration, The Innovation Life 1 (1) (2023) 100015, https://doi.org/10.59717/j.xinn-life.2023.100015.

[10] T. Slanina, P. Šebej, Visible-light-activated photocorms: Rational design of co-releasing organic molecules absorbing in the tissue-transparent window, Photochem. Photobiol. Sci. 17 (6) (2018) 692–710, https://doi.org/10.1039/c8pp00096d.

[11] H.I. Choi, A. Zeb, M.S. Kim, I. Rana, N. Khan, O.S. Qureshi, C.W. Lim, J.S. Park, Z. Gao, H.J. Maeng, J.K. Kim, Controlled therapeutic delivery of co from carbon monoxide-releasing molecules (corms), J. Contr. Release : official journal of the Controlled Release Society 350 (2022) 652–667, https://doi.org/10.1016/j.jconrel.2022.08.055.

[12] S.W. Ryter, K.C. Ma, A.M.K. Choi, Carbon monoxide in lung cell physiology and disease, Am. J. Physiol. Cell Physiol. 314 (2) (2018) C211–C227, https://doi.org/10.1152/ajpcell.00022.2017.

[13] R. Motterlini, L.E. Otterbein, The therapeutic potential of carbon monoxide, Nat. Rev. Drug Discov. 9 (9) (2010) 728–743, https://doi.org/10.1038/nrd3228.

[14] D. Nguyen, C. Boyer, Macromolecular and inorganic nanomaterials scaffolds for carbon monoxide delivery: recent developments and future trends, ACS Biomater. Sci. Eng. 1 (10) (2015) 895–913, https://doi.org/10.1021/acsbiomaterials.5b00230.

[15] J.J. Rose, L. Wang, Q. Xu, C.F. McTiernan, S. Shiva, J. Tejero, M.T. Gladwin, Carbon monoxide poisoning: pathogenesis, management, and future directions of therapy, Am. J. Respir. Crit. Care Med. 195 (5) (2017) 596–606, https://doi.org/10.1164/rccm.201606-1275CI.

[16] C.C. Romao, W.A. Blattler, J.D. Seixas, G.J. Bernardes, Developing drug molecules for therapy with carbon monoxide, Chem. Soc. Rev. 41 (9) (2012) 3571–3583, https://doi.org/10.1039/c2cs15317c.

[17] Y. Zhou, W. Yu, J. Cao, H. Gao, Harnessing carbon monoxide-releasing platforms for cancer therapy, Biomaterials 255 (2020) 120193, https://doi.org/10.1016/j.biomaterials.2020.120193.

[18] A.M. Mansour, R.M. Khaled, E. Khaled, S.K. Ahmed, O.S. Ismael, A. Zeinhom, H. Magdy, S.S. Ibrahim, M. Abdelfatah, Ruthenium(ii) carbon monoxide releasing molecules: structural perspective, antimicrobial and anti-inflammatory properties, Biochem. Pharmacol. 199 (2022) 114991, https://doi.org/10.1016/j.bcp.2022.114991.

[19] H. Yan, J. Du, S. Zhu, G. Nie, H. Zhang, Z. Gu, Y. Zhao, Emerging delivery strategies of carbon monoxide for therapeutic applications: from co gas to co releasing nanomaterials, Small 15 (49) (2019) e1904382, https://doi.org/10.1002/smll.201904382.

[20] Y. Li, Y. Shu, M. Liang, X. Xie, X. Jiao, X. Wang, B. Tang, A two-photon h(2) o(2) -activated co photoreleaser, Angew Chem. Int. Ed. Engl. 57 (38) (2018) 12415–12419, https://doi.org/10.1002/anie.201805806.

[21] X. Jiang, Z. Xiao, W. Zhong, X. Liu, Brief survey of diiron and monoiron carbonyl complexes and their potentials as co-releasing molecules (corms), Coord. Chem. Rev. 429 (2021), https://doi.org/10.1016/j.ccr.2020.213634.

[22] W. Feng, S. Feng, G. Feng, Co release with ratiometric fluorescence changes: a promising visible-light-triggered metal-free co-releasing molecule, Chem. Commun. 55 (61) (2019) 8987–8990, https://doi.org/10.1039/c9cc04026a.

[23] K. Ling, F. Men, W.C. Wang, Y.Q. Zhou, H.W. Zhang, D.W. Ye, Carbon monoxide and its controlled release: therapeutic application, detection, and development of carbon monoxide releasing molecules (corms), J. Med. Chem. 61 (7) (2018) 2611–2635, https://doi.org/10.1021/acs.jmedchem.6b01153.

[24] X. Yang, W. Lu, C.P. Hopper, B. Ke, B. Wang, Nature's marvels endowed in gaseous molecules i: carbon monoxide and its physiological and therapeutic roles, Acta Pharm. Sin. B 11 (6) (2021) 1434–1445, https://doi.org/10.1016/j.apsb.2020.10.010.

[25] L. Rochette, Y. Cottin, M. Zeller, C. Vergely, Carbon monoxide: mechanisms of action and potential clinical implications, Pharmacol. Therapeut. 137 (2) (2013) 133–152, https://doi.org/10.1016/j.pharmthera.2012.09.007.

[26] N. Abeyrathna, K. Washington, C. Bashur, Y. Liao, Nonmetallic carbon monoxide releasing molecules (corms), Org. Biomol. Chem. 15 (41) (2017) 8692–8699, https://doi.org/10.1039/c7ob01674c.

[27] D. Wang, E. Viennois, K. Ji, K. Damera, A. Draganov, Y. Zheng, C. Dai, D. Merlin, B. Wang, A click-and-release approach to co prodrugs, Chem. Commun. 50 (100) (2014) 15890–15893, https://doi.org/10.1039/c4cc07748b.

[28] G.J. Quinlan, A.L. Lagan, T.W. Evans, Haem oxygenase: a model for therapeutic intervention, Intensive Care Med. 34 (4) (2008) 595–597, https://doi.org/10.1007/s00134-008-1013-z.

[29] B.E. Mann, Co-releasing molecules: a personal view, Organometallics 31 (16) (2012) 5728–5735, https://doi.org/10.1021/om300364a.

[30] H. Inaba, K. Fujita, T. Ueno, Design of biomaterials for intracellular delivery of carbon monoxide, Biomater. Sci. 3 (11) (2015) 1423–1438, https://doi.org/10.1039/c5bm00210a.

[31] A.C. Kautz, P.C. Kunz, C. Janiak, Co-releasing molecule (corm) conjugate systems, Dalton transactions (Cambridge, England 45 (45) (2003) 18045–18063, https://doi.org/10.1039/c6dt03515a, 2016.

[32] S. García-Gallego, G.J. Bernardes, Carbon-monoxide-releasing molecules for the delivery of therapeutic co in vivo, Angew Chem. Int. Ed. Engl. 53 (37) (2014) 9712–9721, https://doi.org/10.1002/anie.201311225.

[33] U. Schatzschneider Photocorms, Light-triggered release of carbon monoxide from the coordination sphere of transition metal complexes for biological applications, Inorg. Chim. Acta. 374 (1) (2011) 19–23, https://doi.org/10.1016/j.ica.2011.02.068.

[34] W.-Q. Zhang, A.J. Atkin, R.J. Thatcher, A.C. Whitwood, I.J.S. Fairlamb, J.M. Lynam, Diversity and design of metal-based carbon monoxide-releasing molecules (co-rms) in aqueous systems: revealing the essential trends, Dalton Trans. 22 (2009) 4351–4358, https://doi.org/10.1039/B822157J.

[35] S.O. Alhaj-Suliman, E.I. Wafa, A.K. Salem, Engineering nanosystems to overcome barriers to cancer diagnosis and treatment, Adv. Drug Deliv. Rev. 189 (2022) 114482, https://doi.org/10.1016/j.addr.2022.114482.

[36] S. Huang, X. Ding, Precise design strategies of nanotechnologies for controlled drug delivery, J. Funct. Biomater. 13 (4) (2022) 188, https://doi.org/10.3390/jfb13040188.

[37] W. Mu, Q. Chu, Y. Liu, N. Zhang, A review on nano-based drug delivery system for cancer chemoimmunotherapy, Nano-Micro Lett. 12 (1) (2020) 142, https://doi.org/10.1007/s40820-020-00482-6.

[38] T.G. Dacoba, S. Anthiya, G. Berrecoso, I. Fernández-Mariño, C. Fernández-Varela, J. Crecente-Campo, D. Teijeiro-Osorio, F. Torres Andón, M. J. Alonso Nano-oncologicals, A tortoise trail reaching new avenues, Adv. Funct. Mater. 31 (44) (2021) 2009860, https://doi.org/10.1002/adfm.202009860.

[39] M.J. Mitchell, M.M. Billingsley, R.M. Haley, M.E. Wechsler, N.A. Peppas, R. Langer, Engineering precision nanoparticles for drug delivery, Nat. Rev. Drug Discov. 20 (2) (2021) 101–124, https://doi.org/10.1038/s41573-020-0090-8.

[40] S. Waheed, Z. Li, F. Zhang, A. Chiarini, U. Armato, J. Wu, Engineering nano-drug biointerface to overcome biological barriers toward precision drug delivery, J. Nanobiotechnol. 20 (1) (2022) 395, https://doi.org/10.1186/s12951-022-01605-4.

[41] A.J. Mukalel, R.S. Riley, R. Zhang, M.J. Mitchell, Nanoparticles for nucleic acid delivery: applications in cancer immunotherapy, Cancer Lett. 458 (2019) 102–112, https://doi.org/10.1016/j.canlet.2019.04.040.

[42] A.G. Bhargav, S.K. Mondal, C.A. Garcia, J.J. Green, A. Quiñones-Hinojosa, Nanomedicine revisited: next generation therapies for brain cancer, Adv. Ther. 3 (10) (2020), https://doi.org/10.1002/adtp.202000118.

[43] M.A. Alghamdi, A.N. Fallica, N. Virzì, P. Kesharwani, V. Pittalà, K. Greish, The promise of nanotechnology in personalized medicine, J. Personalized Med. 12 (5) (2022) 673, https://doi.org/10.3390/jpm12050673.

[44] S.M. Kamali Shahri, S. Sharifi, M. Mahmoudi, Interdependency of influential parameters in therapeutic nanomedicine, Expet Opin. Drug Deliv. 18 (10) (2021) 1379–1394, https://doi.org/10.1080/17425247.2021.1921732.

[45] M. Sadeqi Nezhad, Poly (beta-amino ester) as an in vivo nanocarrier for therapeutic nucleic acids, Biotechnol. Bioeng. 120 (1) (2023) 95–113, https://doi.org/10.1002/bit.28269.

[46] J. Karlsson, K.M. Luly, S.Y. Tzeng, J.J. Green, Nanoparticle designs for delivery of nucleic acid therapeutics as brain cancer therapies, Adv. Drug Deliv. Rev. 179 (2021) 113999, https://doi.org/10.1016/j.addr.2021.113999.

[47] Y.M.A. Lau, J. Pang, G. Tilstra, J. Couture-Senécal, O.F. Khan, The engineering challenges and opportunities when designing potent ionizable materials for the delivery of ribonucleic acids, Expet Opin. Drug Deliv. 19 (12) (2022) 1650–1663, https://doi.org/10.1080/17425247.2022.2144827.

[48] G. Vargas-Nadal, M. Köber, A. Nsamela, F. Terenziani, C. Sissa, S. Pescina, F. Sonvico, A.M. Gazzali, H.A. Wahab, L. Grisanti, M.E. Olivera, M.C. Palena, M.L. Guzman, L.C. Luciani-Giacobbe, A. Jimenez-Kairuz, N. Ventosa, I. Ratera, K. D. Belfield, B.M. Maoz, Fluorescent multifunctional organic nanoparticles for drug delivery and bioimaging: a tutorial review, Pharmaceutics 14 (11) (2022) 2498.

[49] T.C. Roberts, R. Langer, M.J.A. Wood, Advances in oligonucleotide drug delivery, Nat. Rev. Drug Discov. 19 (10) (2020) 673–694, https://doi.org/10.1038/s41573-020-0075-7.

[50] N. Singh, J. Kim, J. Kim, K. Lee, Z. Zunbul, I. Lee, E. Kim, S.-G. Chi, J.S. Kim, Covalent organic framework nanomedicines: biocompatibility for advanced nanocarriers and cancer theranostics applications, Bioact. Mater. 21 (2023) 358–380, https://doi.org/10.1016/j.bioactmat.2022.08.016.

[51] R. Sakla, D.A. Jose, Vesicles functionalized with a co-releasing molecule for light-induced co delivery, ACS Appl. Mater. Interfaces 10 (16) (2018) 14214–14220, https://doi.org/10.1021/acsami.8b03310.

[52] U. Schatzschneider Photocorms, Light-triggered release of carbon monoxide from the coordination sphere of transition metal complexes for biological applications, Inorg. Chim. Acta. 374 (1) (2011) 19–23, https://doi.org/10.1016/j.ica.2011.02.068.

[53] R. Sakla, A. Ghosh, V. Kumar, Kanika, P. Das, P.K. Sharma, R. Khan, D.A. Jose, Light activated simultaneous release and recognition of biological signaling molecule carbon monoxide (co), Methods 210 (2023) 44–51, https://doi.org/10.1016/j.ymeth.2023.01.003.

[54] Q. Ouyang, L. Tu, Y. Zhang, H. Chen, Y. Fan, Y. Tu, Y. Li, Y. Sun, Construction of a smart nanofluidic sensor through a redox reaction strategy for high-performance carbon monoxide sensing, Anal. Chem. 92 (22) (2020) 14947–14952, https://doi.org/10.1021/acs.analchem.0c02424.

[55] O. Alghazwat, S. Talebzadeh, J. Oyer, A. Copik, Y. Liao, Ultrasound responsive carbon monoxide releasing micelle, Ultrason. Sonochem. 72 (2021) 105427, https://doi.org/10.1016/j.ultsonch.2020.105427.

[56] B. Liu, X. Zhang, J. Li, S. Yao, Y. Lu, B. Cao, Z. Liu, X-ray-triggered co release based on gdw(10)/mnbr(co)(5) nanomicelles for synergistic radiotherapy and gas therapy, ACS Appl. Mater. Interfaces 14 (6) (2022) 7636–7645, https://doi.org/10.1021/acsami.1c22575.

[57] X. Gao, L. Yan, W. Zhang, Y. Lv, P. Ou, R. Hang, A. Gao, L. Tong, P.K. Chu, H. Wang, Dual-switched carbon monoxide nano gas tank for auto-diagnosis and precision therapy of osteoarthritis, Nano Today 53 (2023) 102047, https://doi.org/10.1016/j.nantod.2023.102047.

[58] S. Oliver, T.T.P. Pham, Y. Li, F.J. Xu, C. Boyer, More than skin deep: using polymers to facilitate topical delivery of nitric oxide, Biomater. Sci. 9 (2) (2021) 391–405, https://doi.org/10.1039/d0bm01197e.

[59] K. Neranon, L. Alberch, O. Ramström, Design, synthesis and self-assembly of functional amphiphilic metallodendrimers, Chemist 9 (1) (2020) 45–52, https://doi.org/10.1002/open.201900298.

[60] A. Salman, A. Kantor, M.E. McClements, G. Marfany, S. Trigueros, R.E. MacLaren, Non-viral delivery of crispr/cas cargo to the retina using nanoparticles: current

possibilities, challenges, and limitations, Pharmaceutics 14 (9) (2022) 1842, https://doi.org/10.3390/pharmaceutics14091842.

[61] J. Yang, C. Jia, J. Yang, Designing nanoparticle-based drug delivery systems for precision medicine, Int. J. Med. Sci. 18 (13) (2021) 2943–2949, https://doi.org/10.7150/ijms.60874.

[62] U. Hasegawa, A.J. van der Vlies, E. Simeoni, C. Wandrey, J.A. Hubbell, Carbon monoxide-releasing micelles for immunotherapy, J. Am. Chem. Soc. 132 (51) (2010) 18273–18280, https://doi.org/10.1021/ja1075025.

[63] D. Nguyen, T.K. Nguyen, S.A. Rice, C. Boyer, Co-releasing polymers exert antimicrobial activity, Biomacromolecules 16 (9) (2015) 2776–2786, https://doi.org/10.1021/acs.biomac.5b00716.

[64] C. Shao, H. Duan, Y. Min, X. Zhang, Diphenyl cyclopropenone-centered polymers for site-specific co-releasing and chain dissociation, Chin. Chem. Lett. 31 (1) (2020) 299–302, https://doi.org/10.1016/j.cclet.2019.03.053.

[65] A.J. van der Vlies, R. Inubushi, H. Uyama, U. Hasegawa, Polymeric framboidal nanoparticles loaded with a carbon monoxide donor via phenylboronic acid-catechol complexation, Bioconjugate Chem. 27 (6) (2016) 1500–1508, https://doi.org/10.1021/acs.bioconjchem.6b00135.

[66] J. Cheng, G. Gan, Z. Shen, L. Gao, G. Zhang, J. Hu, Red light-triggered intracellular carbon monoxide release enables selective eradication of mrsa infection, Angew Chem. Int. Ed. Engl. 60 (24) (2021) 13513–13520, https://doi.org/10.1002/anie.202104024.

[67] J. Cheng, B. Zheng, S. Cheng, G. Zhang, J. Hu, Metal-free carbon monoxide-releasing micelles undergo tandem photochemical reactions for cutaneous wound healing, Chem. Sci. 11 (17) (2020) 4499–4507, https://doi.org/10.1039/d0sc00135j.

[68] U.R. Gandra, A. Sinopoli, S. Moncho, M. NandaKumar, D.B. Ninković, S.D. Zarić, M. Sohail, S. Al-Meer, E.N. Brothers, N.A. Mazloum, M. Al-Hashimi, H.S. Bazzi, Green light-responsive co-releasing polymeric materials derived from ring-opening metathesis polymerization, ACS Appl. Mater. Interfaces 11 (37) (2019) 34376–34384, https://doi.org/10.1021/acsami.9b12628.

[69] M. Zhang, J. Cheng, X. Huang, G. Zhang, S. Ding, J. Hu, R. Qiao, Photo-degradable micelles capable of releasing of carbon monoxide under visible light irradiation, Macromol. Rapid Commun. 41 (18) (2020) e2000323, https://doi.org/10.1002/marc.202000323.

[70] C. Bohlender, S. Gläser, M. Klein, J. Weisser, S. Thein, U. Neugebauer, J. Popp, R. Wyrwa, A. Schiller, Light-triggered co release from nanoporous non-wovens, J. Mater. Chem. B 2 (11) (2014) 1454–1463, https://doi.org/10.1039/c3tb21649g.

[71] S. Gläser, R. Mede, H. Görls, S. Seupel, C. Bohlender, R. Wyrwa, S. Schirmer, S. Dochow, G.U. Reddy, J. Popp, M. Westerhausen, A. Schiller, Remote-controlled delivery of co via photoactive co-releasing materials on a fiber optical device, Dalton Trans. 45 (33) (2016) 13222–13233, https://doi.org/10.1039/c6dt02011a.

[72] A. Chakraborty, P. Dhar, A review on potential of proteins as an excipient for developing a nano-carrier delivery system, Crit. Rev. Ther. Drug Carrier Syst. 34 (5) (2017) 453–488, https://doi.org/10.1615/CritRevTherDrugCarrierSyst.2017018612.

[73] S. Hong, D.W. Choi, H.N. Kim, C.G. Park, W. Lee, H.H. Park, Protein-based nanoparticles as drug delivery systems, Pharmaceutics 12 (7) (2020), https://doi.org/10.3390/pharmaceutics12070604.

[74] M. Fathi, F. Donsi, D.J. McClements, Protein-based delivery systems for the nanoencapsulation of food ingredients, Compr. Rev. Food Sci. Food Saf. 17 (4) (2018) 920–936, https://doi.org/10.1111/1541-4337.12360.

[75] A.O. Elzoghby, M.M. Elgohary, N.M. Kamel, Implications of protein- and peptide-based nanoparticles as potential vehicles for anticancer drugs, Advances in protein chemistry and structural biology 98 (2015) 169–221, https://doi.org/10.1016/bs.apcsb.2014.12.002.

[76] M. Tarhini, H. Greige-Gerges, A. Elaissari, Protein-based nanoparticles: from preparation to encapsulation of active molecules, Int. J. Pharm. 522 (1–2) (2017) 172–197, https://doi.org/10.1016/j.ijpharm.2017.01.067.

[77] A. Jain, S.K. Singh, S.K. Arya, S.C. Kundu, S. Kapoor, Protein nanoparticles: promising platforms for drug delivery applications, ACS Biomater. Sci. Eng. 4 (12) (2018) 3939–3961, https://doi.org/10.1021/acsbiomaterials.8b01098.

[78] A.O. Elzoghby, W.M. Samy, N.A. Elgindy, Protein-based nanocarriers as promising drug and gene delivery systems, J. Contr. Release : official journal of the Controlled Release Society 161 (1) (2012) 38–49, https://doi.org/10.1016/j.jconrel.2012.04.036.

[79] H. Pfeiffer, T. Sowik, U. Schatzschneider, Bioorthogonal oxime ligation of a mo (co)4(n–n) co-releasing molecule (corm) to a tgf β-binding peptide, J. Organomet. Chem. 734 (2013) 17–24, https://doi.org/10.1016/j.jorganchem.2012.09.016.

[80] K. Fujita, Y. Tanaka, S. Abe, T. Ueno, A photoactive carbon-monoxide-releasing protein cage for dose-regulated delivery in living cells, Angew Chem. Int. Ed. Engl. 55 (3) (2016) 1056–1060, https://doi.org/10.1002/anie.201506738.

[81] H. Inaba, N.J. Sanghamitra, K. Fujita, T. Sho, T. Kuchimaru, S. Kitagawa, S. Kizaka-Kondoh, T. Ueno, A metal carbonyl-protein needle composite designed for intracellular co delivery to modulate nf-κb activity, Mol. Biosyst. 11 (11) (2015) 3111–3118, https://doi.org/10.1039/c5mb00327j.

[82] H. Tabe, K. Fujita, S. Abe, M. Tsujimoto, T. Kuchimaru, S. Kizaka-Kondoh, M. Takano, S. Kitagawa, T. Ueno, Preparation of a cross-linked porous protein crystal containing ru carbonyl complexes as a co-releasing extracellular scaffold, Inorg. Chem. 54 (1) (2015) 215–220, https://doi.org/10.1021/ic502159x.

[83] I. Kim, E.H. Han, W.-Y. Bang, J. Ryu, J.-Y. Min, H.C. Nam, W.H. Park, Y.-H. Chung, E. Lee, Supramolecular carbon monoxide-releasing peptide hydrogel patch, Adv. Funct. Mater. 28 (47) (2018) 1803051, https://doi.org/10.1002/adfm.201803051.

[84] L. Wu, X. Cai, H. Zhu, J. Li, D. Shi, D. Su, D. Yue, Z. Gu, PDT-driven highly efficient intracellular delivery and controlled release of co in combination with sufficient singlet oxygen production for synergistic anticancer therapy, Adv. Funct. Mater. 28 (41) (2018) 1804324, https://doi.org/10.1002/adfm.201804324.

[85] Y. Zeng, M. Fan, Q. Zhou, D. Chen, T. Jin, Z. Mu, L. Li, J. Chen, D. Qiu, Y. Zhang, Y. Pan, X. Shen, X. Cai, Reactive oxygen species-activated CO versatile nanomedicine with innate gut immune and microbiome remodeling effects for treating inflammatory bowel disease, Adv. Funct. Mater. 33 (49) (2023) 2304381, https://doi.org/10.1002/adfm.202304381.

[86] D. Zhong, Z. Tu, X. Zhang, Y. Li, X. Xu, Z. Gu, Bioreducible peptide-dendrimeric nanogels with abundant expanded voids for efficient drug entrapment and delivery, Biomacromolecules 18 (11) (2017) 3498–3505, https://pubs.acs.org/doi/10.1021/acs.biomac.7b00649.

[87] X. Cai, J. Tian, J. Zhu, J. Chen, L. Li, C. Yang, J. Chen, D. Chen, Photodynamic and photothermal co-driven CO-enhanced multi-mode synergistic antibacterial nanoplatform to effectively fight against biofilm infections, Chem. Eng. J. 426 (2020) 131919, https://doi.org/10.1016/j.cej.2021.131919.

[88] G. Yang, M. Fan, J. Zhu, C. Ling, L. Wu, X. Zhang, M. Zhang, J. Li, Q. Yao, Z. Gu, X. Cai, A multifunctional anti-inflammatory drug that can specifically target activated macrophages, massively deplete intracellular H2O2, and produce large amounts CO for a highly efficient treatment of osteoarthritis, Biomaterials 255 (2020) 120155, https://doi.org/10.1016/j.biomaterials.2020.120155.

[89] M. Popova, L.S. Lazarus, S. Ayad, A.D. Benninghoff, L.M. Berreau, Visible-light-activated quinolone carbon-monoxide-releasing molecule: prodrug and albumin-assisted delivery enables anticancer and potent anti-inflammatory effects, J. Am. Chem. Soc. 140 (30) (2018) 9721–9729, https://doi.org/10.1021/jacs.8b06011.

[90] Y. Zhou, Y. Sun, K. Yi, Z. Wang, Y. Liu, C. He, Solid-phase synthesis of peptides with azopyridine side-chains for mn(i)-co binding and red-light responsive co release, Inorg. Chem. Front. 9 (22) (2022) 5941–5949, https://doi.org/10.1039/d2qi01653b.

[91] L. Feng, K.Y. Wang, G.S. Day, M.R. Ryder, H.C. Zhou, Destruction of metal-organic frameworks: positive and negative aspects of stability and lability, Chem. Rev. 120 (23) (2020) 13087–13133, https://doi.org/10.1021/acs.chemrev.0c00722.

[92] J. Wu, Y. Yu, Y. Cheng, C. Cheng, Y. Zhang, B. Jiang, X. Zhao, L. Miao, H. Wei, Ligand-dependent activity engineering of glutathione peroxidase-mimicking mil-47(v) metal-organic framework nanozyme for therapy, Angew Chem. Int. Ed. Engl. 60 (3) (2021) 1227–1234, https://doi.org/10.1002/anie.202010714.

[93] J. Cao, X. Li, H. Tian, Metal-organic framework (mof)-based drug delivery, Curr. Med. Chem. 27 (35) (2020) 5949–5969, https://doi.org/10.2174/0929867326666190618152518.

[94] N.A. Khan, Z. Hasan, S.H. Jhung, Adsorptive removal of hazardous materials using metal-organic frameworks (mofs): a review, J. Hazard Mater. 244–245 (2013) 444–456, https://doi.org/10.1016/j.jhazmat.2012.11.011.

[95] W. Chen, C. Wu Synthesis, functionalization, and applications of metal-organic frameworks in biomedicine, Dalton transactions (Cambridge, England : 2003 47 (7) (2018) 2114–2133, https://doi.org/10.1039/c7dt04116k.

[96] J. Chen, D. Sheng, T. Ying, H. Zhao, J. Zhang, Y. Li, H. Xu, S. Chen, Mofs-based nitric oxide therapy for tendon regeneration, Nano-Micro Lett. 13 (1) (2020) 23, https://doi.org/10.1007/s40820-020-00542-x.

[97] Y. Li, B. Zou, A. Xiao, H. Zhang, Advances of metal-organic frameworks in energy and environmental applications, Chin. J. Chem. 35 (10) (2017) 1501–1511, https://doi.org/10.1002/cjoc.201700151.

[98] Z. Zhai, X. Zhang, X. Hao, B. Niu, C. Li, Metal-organic frameworks materials for capacitive gas sensors, Adv Mater Technol 6 (10) (2021) 2100127, https://doi.org/10.1002/admt.202100127.

[99] S. Ren, H. Yu, L. Wang, Z. Huang, T. Lin, Y. Huang, J. Yang, Y. Hong, J. Liu. State of the art and prospects in metal-organic framework-derived microwave absorption materials, Nano-Micro Lett. 14 (1) (2022) 68, https://doi.org/10.1007/s40820-022-00808-6.

[100] E. Martínez-Ahumada, A. López-Olvera, V. Jancik, J.E. Sánchez-Bautista, E. González-Zamora, V. Martis, D.R. Williams, I.A. Ibarra, Mof materials for the capture of highly toxic h2s and so2, Organometallics 39 (7) (2020) 883–915, https://doi.org/10.1021/acs.organomet.9b00735.

[101] K. Vellingiri, A. Deep, K.-H. Kim, Metal-organic frameworks as a potential platform for selective treatment of gaseous sulfur compounds, ACS Appl. Mater. Interfaces 8 (44) (2016) 29835–29857, https://doi.org/10.1021/acsami.6b10482.

[102] Y. Sun, L. Zheng, Y. Yang, X. Qian, T. Fu, X. Li, Z. Yang, H. Yan, C. Cui, W. Tan, Metal-organic framework nanocarriers for drug delivery in biomedical applications, Nano-Micro Lett. 12 (1) (2020) 103, https://doi.org/10.1007/s40820-020-00423-3.

[103] D. Li, H.-Q. Xu, L. Jiao, H.-L. Jiang, Metal-organic frameworks for catalysis: state of the art, challenges, and opportunities, Inside Energy 1 (1) (2019) 100005, https://doi.org/10.1016/j.enchem.2019.100005.

[104] Y. Li, Z. Liu, W. Zeng, Z. Wang, C. Liu, N. Zeng, K. Zhong, D. Jiang, Y. Wu, A novel h(2)o(2) generator for tumor chemotherapy-enhanced co gas therapy, Front. Oncol. 11 (2021) 738567, https://doi.org/10.3389/fonc.2021.738567.

[105] M. Ma, H. Noei, B. Mienert, J. Niesel, E. Bill, M. Muhler, R.A. Fischer, Y. Wang, U. Schatzschneider, N. Metzler-Nolte, Iron metal-organic frameworks mil-88b and nh2-mil-88b for the loading and delivery of the gasotransmitter carbon monoxide, Chem. Eur. J. 19 (21) (2013) 6785–6790, https://doi.org/10.1002/chem.201201743.

[106] Y. Mu, W. Li, X. Yang, J. Chen, Y. Weng, Partially reduced mil-100(fe) as a co carrier for sustained co release and regulation of macrophage phenotypic

polarization, ACS Biomater. Sci. Eng. 8 (11) (2022) 4777–4788, https://doi.org/10.1021/acsbiomaterials.2c00959.

[107] S. Diring, A. Carné-Sánchez, J. Zhang, S. Ikemura, C. Kim, H. Inaba, S. Kitagawa, S. Furukawa, Light responsive metal-organic frameworks as controllable co-releasing cell culture substrates, Chem. Sci. 8 (3) (2017) 2381–2386, https://doi.org/10.1039/c6sc04824b.

[108] F.J. Carmona, S. Rojas, C.C. Romão, J.A.R. Navarro, E. Barea, C.R. Maldonado, One-pot preparation of a novel co-releasing material based on a co-releasing molecule@metal-organic framework system, Chem. Commun. 53 (49) (2017) 6581–6584, https://doi.org/10.1039/c7cc03605a.

[109] F.J. Carmona, C.R. Maldonado, S. Ikemura, C.C. Romão, Z. Huang, H. Xu, X. Zou, S. Kitagawa, S. Furukawa, E. Barea, Coordination modulation method to prepare new metal-organic framework-based co-releasing materials, ACS Appl. Mater. Interfaces 10 (37) (2018) 31158–31167, https://doi.org/10.1021/acsami.8b11758.

[110] A.F. Silva, I.B. Calhau, A.C. Gomes, A.A. Valente, I.S. Gonçalves, M. Pillinger, A hafnium-based metal-organic framework for the entrapment of molybdenum hexacarbonyl and the light-responsive release of the gasotransmitter carbon monoxide, Mater. Sci. Eng. C 124 (2021) 112053, https://doi.org/10.1016/j.msec.2021.112053.

[111] Z. Jin, P. Zhao, J. Zhang, T. Yang, G. Zhou, D. Zhang, T. Wang, Q. He, Intelligent metal carbonyl metal-organic framework nanocomplex for fluorescent traceable h2o2 -triggered co delivery, Chemistry 24 (45) (2018) 11667–11674, https://doi.org/10.1002/chem.201801407.

[112] J. Seaberg, H. Montazerian, M.N. Hossen, R. Bhattacharya, A. Khademhosseini, P. Mukherjee, Hybrid nanosystems for biomedical applications, ACS Nano 15 (2) (2021) 2099–2142, https://doi.org/10.1021/acsnano.0c09382.

[113] X. Li, J. Tsiboulkis, T. Weng, B. Zhang, G. Yin, G. Feng, Y. Cui, I.N. Savina, L. I. Mikhalovska, S.R. Sandeman, C.A. Howel, S.V. Mikhalovsky, Nano carriers for drug transport across the blood-brain barrier, J. Drug Target. 25 (1) (2017) 17–28, https://doi.org/10.1080/1061186x.2016.1184272.

[114] L. Yang, E.S. Feura, M.J.R. Ahonen, M.H. Schoenfisch, Nitric oxide-releasing macromolecular scaffolds for antibacterial applications, Adv. Healthcare Mater. 7 (13) (2018) e1800155, https://doi.org/10.1002/adhm.201800155.

[115] L. Guo, N. He, Y. Zhao, T. Liu, Y. Deng, Autophagy modulated by inorganic nanomaterials, Theranostics 10 (7) (2020) 3206–3222, https://doi.org/10.7150/thno.40414.

[116] F.J. Carmona, S. Rojas, P. Sánchez, H. Jeremias, A.R. Marques, C.C. Romão, D. Choquesillo-Lazarte, J.A. Navarro, C.R. Maldonado, E. Barea, Cation exchange strategy for the encapsulation of a photoactive co-releasing organometallic molecule into anionic porous frameworks, Inorg. Chem. 55 (13) (2016) 6525–6531, https://doi.org/10.1021/acs.inorgchem.6b00674.

[117] F.J. Carmona, I. Jiménez-Amezcua, S. Rojas, C.C. Romão, J.A.R. Navarro, C. R. Maldonado, E. Barea, Aluminum doped mcm-41 nanoparticles as platforms for the dual encapsulation of a co-releasing molecule and cisplatin, Inorg. Chem. Front. 56 (17) (2017) 10474–10480, https://doi.org/10.1021/acs.inorgchem.7b01475.

[118] J. Wu, Z. Meng, A.A. Exner, X. Cai, X. Xie, B. Hu, Y. Chen, Y. Zheng, Biodegradable cascade nanocatalysts enable tumor-microenvironment remodeling for controllable co release and targeted/synergistic cancer nanotherapy, Biomaterials 276 (2021) 121001, https://doi.org/10.1016/j.biomaterials.2021.121001.

[119] S. Zheng, P. Dou, S. Jin, M. Jiao, W. Wang, Z. Jin, Y. Wang, J. Li, K. Xu, Tumor microenvironment/nir-responsive carbon monoxide delivery with hollow mesoporous cus nanoparticles for mr imaging guided synergistic therapy, Mater. Des. 205 (2021) 109731, https://doi.org/10.1016/j.matdes.2021.109731.

[120] W.P. Li, C.H. Su, L.C. Tsao, C.T. Chang, Y.P. Hsu, C.S. Yeh, Controllable co release following near-infrared light-induced cleavage of iron carbonyl derivatized prussian blue nanoparticles for co-assisted synergistic treatment, ACS Nano 10 (12) (2016) 11027–11036, https://doi.org/10.1021/acsnano.6b05858.

[121] S.B. Wang, C. Zhang, J.J. Ye, M.Z. Zou, C.J. Liu, X.Z. Zhang, Near-infrared light responsive nanoreactor for simultaneous tumor photothermal therapy and carbon monoxide-mediated anti-inflammation, ACS Cent. Sci. 6 (4) (2020) 555–565, https://doi.org/10.1021/acscentsci.9b01342.

[122] G. Dördelmann, T. Meinhardt, T. Sowik, A. Krueger, U. Schatzschneider, Cuaac click functionalization of azide-modified nanodiamond with a photoactivatable co-releasing molecule (photocorm) based on [mn(co)3(tpm)]+, Chem. Commun. 48 (94) (2012) 11528–11530, https://doi.org/10.1039/c2cc36491c.

[123] I.B. Calhau, A.C. Gomes, S.M. Bruno, A.C. Coelho, C.I.R. Magalhães, C.C. Romão, A.A. Valente, I.S. Gonçalves, M. Pillinger, One-pot intercalation strategy for the encapsulation of a co-releasing organometallic molecule in a layered double hydroxide, Eur. J. Inorg. Chem. 2020 (28) (2020) 2726–2736, https://doi.org/10.1002/ejic.202000202.

[124] P.C. Kunz, H. Meyer, J. Barthel, S. Sollazzo, A.M. Schmidt, C. Janiak, Metal carbonyls supported on iron oxide nanoparticles to trigger the co-gasotransmitter release by magnetic heating, Chem. Commun. 49 (43) (2013) 4896–4898, https://doi.org/10.1039/c3cc41411f.

[125] H. Meyer, F. Winkler, P. Kunz, A.M. Schmidt, A. Hamacher, M.U. Kassack, C. Janiak, Stabilizing alginate confinement and polymer coating of co-releasing molecules supported on iron oxide nanoparticles to trigger the co release by magnetic heating, Inorg. Chem. 54 (23) (2015) 11236–11246, https://doi.org/10.1021/acs.inorgchem.5b01675.

[126] H. Meyer, M. Brenner, S.-P. Höfert, T.-O. Knedel, P.C. Kunz, A.M. Schmidt, A. Hamacher, M.U. Kassack, C. Janiak, Synthesis of oxime-based co-releasing molecules, corms and their immobilization on maghemite nanoparticles for magnetic-field induced co release, Dalton Trans. 45 (18) (2016) 7605–7615, https://doi.org/10.1039/C5DT04888E.

[127] J. Ou, W. Zheng, Z. Xiao, Y. Yan, X. Jiang, Y. Dou, R. Jiang, X. Liu, Core-shell materials bearing iron(ii) carbonyl units and their co-release via an upconversion process, J. Mater. Chem. B 5 (41) (2017) 8161–8168, https://doi.org/10.1039/c7tb01434a.

[128] C. Liu, Z. Du, M. Ma, Y. Sun, J. Ren, X. Qu, Carbon monoxide controllable targeted gas therapy for synergistic anti-inflammation, iScience 23 (9) (2020) 101483, https://doi.org/10.1016/j.isci.2020.101483.

[129] Q. Dai, L. Wang, E. Ren, H. Chen, X. Gao, H. Cheng, Y. An, C. Chu, G. Liu, Ruthenium-based metal-organic nanoradiosensitizers enhance radiotherapy by combining ros generation and co gas release, Angew Chem. Int. Ed. Engl. 61 (50) (2022) e202211674, https://doi.org/10.1002/anie.202211674.

[130] A.R. Fernandes, I. Mendonça-Martins, M.F.A. Santos, L.R. Raposo, R. Mendes, J. Marques, C.C. Romão, M.J. Romão, T. Santos-Silva, P.V. Baptista, Improving the anti-inflammatory response via gold nanoparticle vectorization of co-releasing molecules, ACS Biomater. Sci. Eng. 6 (2) (2020) 1090–1101, https://doi.org/10.1021/acsbiomaterials.9b01936.

[131] A.E. Pierri, P.J. Huang, J.V. Garcia, J.G. Stanfill, M. Chui, G. Wu, N. Zheng, P. C. Ford, A photocorm nanocarrier for co release using nir light, Chem. Commun. 51 (11) (2015) 2072–2075, https://doi.org/10.1039/c4cc06766e.

[132] C. Steiger, C. Hermann, L. Meinel, Localized delivery of carbon monoxide, Eur. J. Pharm. Biopharm. 118 (2017) 3–12, https://doi.org/10.1016/j.ejpb.2016.11.002.

[133] P. Wang, H. Liu, Q. Zhao, Y. Chen, B. Liu, B. Zhang, Q. Zheng, Syntheses and evaluation of drug-like properties of co-releasing molecules containing ruthenium and group 6 metal, Eur. J. Med. Chem. 74 (2014) 199–215, https://doi.org/10.1016/j.ejmech.2013.12.041.

[134] M. Faizan, N. Muhammad, K.U.K. Niazi, Y. Hu, Y. Wang, Y. Wu, H. Sun, R. Liu, W. Dong, W. Zhang, Z. Gao, Co-releasing materials: an emphasis on therapeutic implications, as release and subsequent cytotoxicity are the part of therapy, Materials 12 (10) (2019) 1643, https://doi.org/10.3390/ma12101643.

[135] X.X. Yang, B.W. Ke, W. Lu, B.H. Wang, Co as a therapeutic agent: discovery and delivery forms, Chin. J. Nat. Med. 18 (4) (2020) 284–295, https://doi.org/10.1016/S1875-5364(20)30036-4.

[136] S.H. Heinemann, T. Hoshi, M. Westerhausen, A. Schiller, Carbon monoxide-physiology, detection and controlled release, Chem. Commun. 50 (28) (2014) 3644–3660, https://doi.org/10.1039/c3cc49196j.

[137] N. Yang, W. Xiao, X. Song, W. Wang, X. Dong, Recent advances in tumor microenvironment hydrogen peroxide-responsive materials for cancer photodynamic therapy, Nano-Micro Lett. 12 (1) (2020) 15, https://doi.org/10.1007/s40820-019-0347-0.

[138] C. Marín-Hernández, A. Toscani, F. Sancenón, J.D.E.T. Wilton-Ely, R. Martínez-Máñez, Chromo-fluorogenic probes for carbon monoxide detection, Chem. Commun. 52 (35) (2016) 5902–5911, https://doi.org/10.1039/C6CC01335J.

[139] X. Liu, N. Li, M. Li, H. Chen, N. Zhang, Y. Wang, K. Zheng, Recent progress in fluorescent probes for detection of carbonyl species: formaldehyde, carbon monoxide and phosgene, Coord. Chem. Rev. 404 (2020) 213109, https://doi.org/10.1016/j.ccr.2019.213109.